Carbonates and Evaporites (2019) 34:623–656
https://doi.org/10.1007/s13146-018-0430-5

ORIGINAL ARTICLE

Microfacies and diagenetic studies of the early Eocene Sakesar Limestone, Potwar Plateau, Pakistan: approach of reservoir evaluation using outcrop analogue

Muhammad Ishaq[1,2] · Irfan U. Jan[2] · Muhammad Hanif[2] · Muhammad Awais[1]

Accepted: 28 January 2018 / Published online: 10 February 2018

Abstract
The early Eocene Sakesar Limestone of the Salt Range has been investigated in detail for microfacies analysis, depositional modeling, diagenesis and reservoir characterization. This research work was comprised of two outcrop sections, i.e., Nilawahan Gorge Section (NGS) and Katas Temple Sections (KTS) of the Sakesar Limestone, central and eastern Salt Range, Potwar Plateau. This work is mainly concentrated on investigating and evaluating the reservoir quality through depositional and diagenetic fabrics. The depositional, diagenetic and deformational processes are controlling factors of porosity and permeability distribution. On the basis of relative estimated ratio of allochemical constituents and micrite, five microfacies have been recognized. These microfacies are: Benthonic Foraminiferal wackestone, Foraminiferal-Algal wackestone–packstone, Miliolidal-Algal wackestone–packstone, Nummulitic-Assilina Packstone and Alveolina-Algal packstone. On the basis of relative abundance of biota, their associations and the presence of micritic matrix in various microfacies, the Sakesar Limestone is interpreted to be deposited in the proximal inner ramp to middle ramp settings. The Sakesar Limestone is largely affected and modified by various diagenetic events which have destroyed primary nature of reservoir and developed it as prolific secondary reservoir. The paragenetic sequence includes micritization, cementation, dissolution, neomorphism, nodularity, silicification, mechanical compaction, stylolitization, fractures and veins formation. The identified porosity types include intraparticle, intercrystalline, moldic, cavernous and fracture. The visually estimated average micro porosities of the Sakesar Limestone vary between 0.5 and 2.1% in the NGS and KTS. The core plug porosity and permeability of outcrop samples vary between 0.9 and 2.9%. The relation of core plug porosity and permeability has moderate positive correlation coefficient. The fractures and dissolution on microscopic and macroscopic level are the dominant factors that enhance the reservoir potentiality of the Sakesar Limestone.

Keywords Microfacies · Diagenesis · Reservoir · Sakesar Limestone · Potwar Plateau · Pakistan

Introduction

The Potwar Plateau is an important area for hydrocarbon exploration, Attock Oil Company first discovered oil in the Khaur Field in 1914 (Fig. 1a; Khan et al. 1986). Successive discoveries comprised the Khaur (1914), Dhulian (1935), Balkassar (1944), Joya Mair (1945), Karsal (1956), Meyal (1968), Toot (1968), Adhi (1978), Dakhni (1983) and Dhurnal (1984) fields (Khan et al. 1986). The Oil and Gas Development Company Limited (OGDCL) discovered oil at Fimkassar in 1989 (Fig. 1a; Khan et al. 1986). The investigated outcrop sections are part of the Salt Range, Potwar Plateau, Pakistan.

The early Eocene strata is well exposed in the Salt Range and Trans-Indus Range that include Nammal Formation, Sakesar Limestone, Chorgali Formation (Fig. 1a; Gee and Gee 1989). In the Salt Range, Davies and Pinfold (1937) established the marine Paleogene stratigraphy and demonstrated the age-diagnostic larger benthonic foraminifera. They also described the lithology of the Sakesar Limestone which in places consisted of light to dark gray and in places creamy, thin- to thick-bedded massive nodular

✉ Muhammad Ishaq
geoishaq88@gmail.com

[1] Department of Geology, University of Swabi, Swabi 23561, Pakistan

[2] National Centre of Excellence in Geology, University of Peshawar, Peshawar 25130, Pakistan

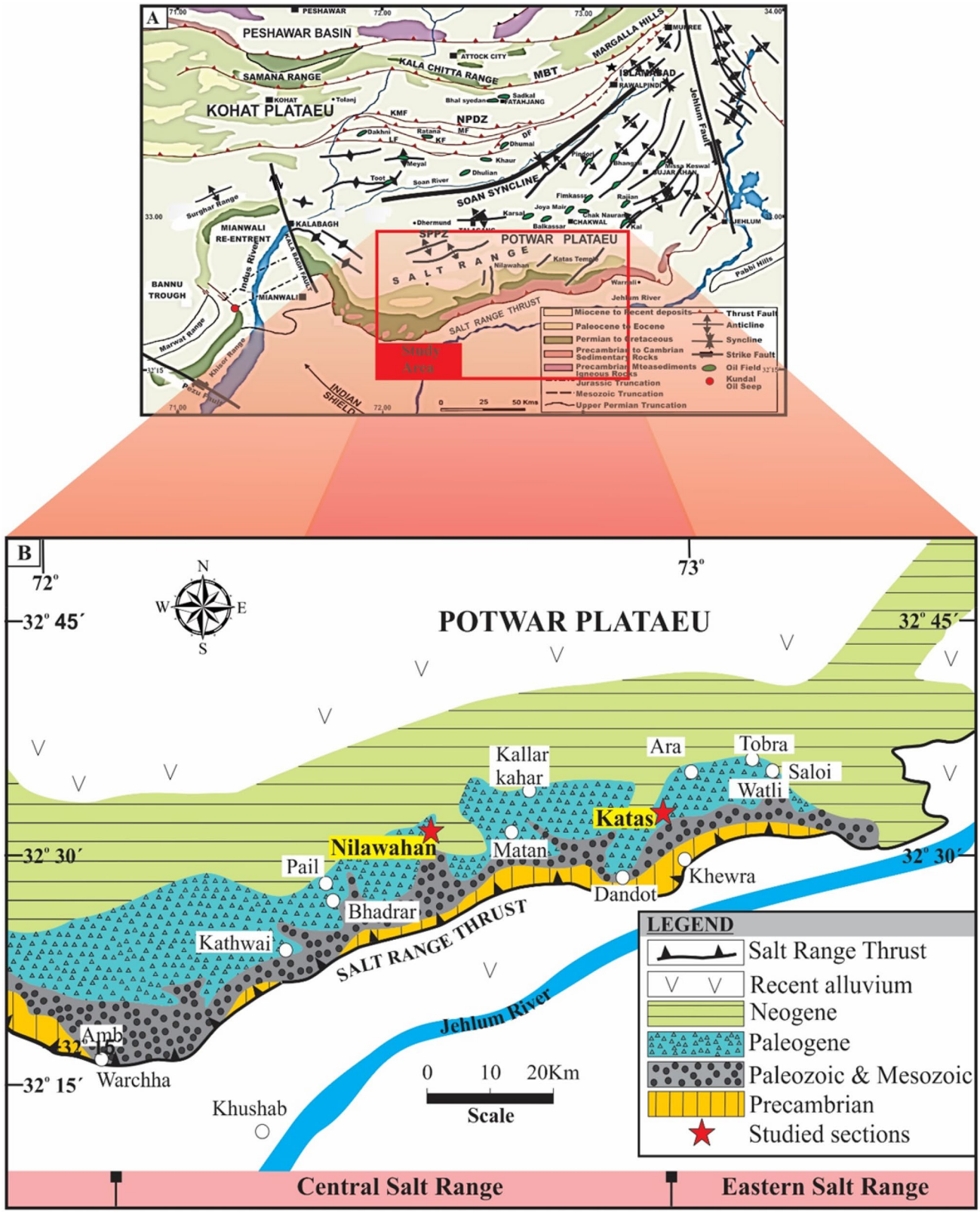

Fig. 1 **a** Generalized geologic and tectonic map of the Salt Range-Potwar Foreland Basin, showing the location of oil/gas structures (modified after Khan et al. 1986; Jaswal et al. 1997). The structural features are: *DF* Dhurnal fault, *KF* Kanet fault, *KMF* Khair-e-Murat fault, *LF* Langrial fault, *MBT* main boundary thrust, *NPDZ* North Potwar Deformed Zone, *SPPZ* South Potwar Platform Zone. **b** Location map of Nilawahan Gorge and Katas Temple sections, Central and Eastern Salt Range, respectively, Potwar Plateau (Modified from Jan and Stephenson 2011; Ghazi et al. 2015)

limestone which is cherty in the upper part. It is mainly fossiliferous and contains corals, mollusks and larger benthonic foraminifera (Davies and Pinfold 1937). Several people have established microfacies of the Sakesar Limestone from central Salt Range and concluded that there were two main microfacies, i.e., packstone and wackestone, which were divided into sub-microfacies based on the dominant bioclasts and interpreted restricted lagoonal depositional setting. Subsequent work (Boustani and Khwaja 1997; Afzal and Butt 2000; Sameeni and Butt 2004; Ghazi et al. 2006, 2010; Nizami et al. 2010; Ahmad et al. 2013) also dealt with sedimentology and biostratigraphy of the Sakesar Limestone from different parts of Salt Range. They delineated different microfacies such as bioclastic packstone, wackestone and wackestone to packstone. The microfacies showed cyclicity as these zones repeated at certain stratigraphic levels (Ghazi et al. 2010). The biostratigraphic findings revealed that the Sakesar Limestone is hosting a number of biostratigraphically important larger benthonic foraminiferal species belonging to the genera: *Nummulites, Assilina, Lockhartia, Alveolina* and *Opercolina* along with brachiopods, gastropods, pelecypods, echinoderms, bryozoa, sponges, corals, blue-green Algae and Red Algae. The diagenetic characteristics of the Sakesar Limestone include stylolitization, calcitization, silicification, nodularity, dissolution, replacement, dolomitization, micritization, various cement morphologies, micritic envelopes, open and filled fractures (calcite veins) and dissolution. The hydrocarbon exploration in the Potwar Plateau focuses on shallow-lying Eocene and Paleocene successions that have proved conventional productive reservoir intervals mainly producing from fractures (Mujtaba and Abbas 2001; Jadoon et al. 2005). The Eocene Sakesar Limestone also forms a portion of these shallow-lying reservoir intervals frequently exploited for hydrocarbon (Jadoon et al. 2005).

The present work has taken the consideration of reservoir evaluation of the Sakesar Limestone which is one of the major and proven reservoir in many oil/gas fields of the Potwar Plateau (Aamir and Siddiqui 2006). The present research utilizes outcrop sections from central and eastern Salt Range to investigate surface petrographical and sedimentological aspects to investigate reservoir properties of the Sakesar Limestone. The NGS (Fig. 1b; N32°39′08.3″, E72°35′56.7″) is exposed on the Khushab Road, Noor Pur Village, central Salt Range and the KTS (Fig. 1b; N32°43′28.5″, E72°57′25.8″) is exposed on the Kallar Kahar Road, Choa Saidan Shah, eastern Salt Range, Potwar Plateau.

The objectives of the present study include to understand and interpret the microfacies of the Sakesar Limestone in the selected outcrop sections and proposed a depositional model; to understand various diagenetic processes, their paragenetic sequence and proposed a diagenetic model for the Sakesar Limestone; and to delineate origin, type and amount of porosity, permeability and the impact of diagenesis on the reservoir quality and potentiality. The present study may be helpful in the future development of the Sakesar Limestone as hydrocarbon reservoir either in some undiscovered oil/gas fields or to extend the limits of already discovered fields.

General geology of the study area

The Himalayan collision between Indian and Asian plates resulted in the development of several foreland basins in Pakistan and India (Acharyya 2007). The Salt Range/Potwar Plateau (SRPP) is one of the manifestations of this globally famous and distinct Himalayan collision (Fig. 1a). The SRPP forms the active fold and thrust belts of Himalayan foreland in north Pakistan which comprised approximately 130 km wide deformed zone (Jaswal et al. 1997). Structurally, the SRPP constitutes four main tectonic zones from north to south, i.e., the Northern Potwar Deformed Zone (NPDZ; Jaswal et al. 1997; Jadoon et al. 2008), Soan Syncline, the Southern Potwar Platform Zone (SPPZ; Shami and Baig 2002) and the Salt Range (Gee 1980). The intensely deformed NPDZ is a contraction zone bounded by MBT to the north, the Soan Syncline to the south, Jehlum Fault to the east and Indus River to west (Fig. 1a). The prominent tectonic features of the NPDZ are Khair-e-Murat Fault, Kanet Fault, Langrial Fault and Dhurnal Fault while Khaur, Dhulian, Dhumal, Meyal, Toot, Ratana, Bhal Syedan and Sadkal are the most efficient anticlinal structures producing oil and gas in the NPDZ (Fig. 1a). The Soan Syncline is zone between intensely deformed NDPZ to north and relatively undeformed South Potwar Platform Zone (SPPZ) to the south (Fig. 1a). The SPPZ is bounded by the right lateral Kalabagh Fault to the west, Salt Range to the South, left lateral Jehlum Fault to east and Soan Syncline to north (Jadoon et al. 2008). The Salt Range is essentially a complex anticlinorium structure with a series of salt anticlines trending east-northeast through northern Pakistan (Sarwar and DeJong 1979; Gee and Gee 1989; Fig. 1a). The Salt Range exposes a wide spectrum of sedimentary successions from the Precambrian to Quaternary (except Ordovician to Carboniferous) along the Salt Range Thrust (Kazmi and Jan 1997).

Materials and methods

For the present research work, two stratigraphic sections of the Sakesar Limestone were measured and logged at NGS and KTS, Salt Range (Fig. 1b). The stratigraphic logging was carried out using conventional methods. All field features of the Sakesar Limestone were observed and noted at the outcrop scale that includes textural and

lithological variations, diagenetic features, nature of bedding, color, etc. From both stratigraphic sections, representative carbonate samples were collected in systematic manner. Blue dyed thin sections were prepared at Rock cutting laboratory, NCE in Geology, University of Peshawar. The classical optical microscopy was utilized for microfacies analysis, diagenesis and reservoir characterization on microscopic scale and, subsequently, inventories were made for microfacies analysis, diagenetic features and their relative chronology and reservoir characteristics of the Sakesar Limestone. The petrographic microfacies of carbonate is constructed on Dunham limestone classification (Dunham 1962). Flügel (2010) microfacies belts and microfacies models were also used.

The Scanning Electron Microscope (SEM) at Centralized Resource Laboratory at Department of Physics, University of Peshawar was used for the micritic sediments and high-resolution photomicrographs to elucidate various porosity types and diagenetic aspects of the Sakesar Limestone. The core plugs were prepared and analyzed for quantitative measurements of porosity and permeability at the Hydrocarbon Development Institute of Pakistan (HDIP), Islamabad. The porosity and permeability test of plug samples performed at an overburden pressure of 500 and 400 psi, respectively.

Results

Lithostratigraphy of Sakesar Limestone

The Eocene Sakesar Limestone is widely distributed in Potwar Plateau. The lithologic units of the Sakesar Limestone have been delineated in the NGS and KTS (Figs. 2, 3). At the NGS, the Sakesar Limestone is predominantly composed of nodular limestone with marl and shale in subordinate amount (Fig. 2). The limestone is dark grayish and pale-yellow to cream colored on the weathered surface and light gray to gray colored on the fresh surface. Marls are light gray to white while shale is gray in color. The lower part of the formation is thick bedded while in the upper horizons of the formation the bedding becomes massive. The size of limestone nodules is 30–70 cm in the lower part of the formation and in the middle part of the formation the size of the nodules decreases to 15–30 cm. The diameter of the chert nodules is mostly in the range of 5–10 cm and occasionally up to 60 cm in diameter. The thickness of the formation is 75 m at the NGS and 19.5 m at the KTS where the basal part of the formation is not exposed (Figs. 2, 3). On the basis of lithological variations, the Sakesar Limestone at the NGS can be divided into the following three lithostratigraphic units;

Lower Limestone unit with subordinate shales and marls

This unit is 17 m thick which is composed of limestone, shale and marls (Fig. 4a). The gray color, thick bedded, fossiliferous and nodular limestone is interbedded with thin shales and marls. The nodules of limestone range from 30 to 70 cm in diameter. Occasionally large chert nodules are found (Fig. 4b).

Middle nodular limestone unit with marls

This unit is 35.3 m thick. This limestone unit is compact and fossiliferous as compared to lower unit. As compared to the lower limestone unit, here limestone nodules are smaller in size and interbedded with marls (Fig. 4c). The limestone is yellowish white to gray on weathered surface and grayish on fresh surface. The bedding is wavy to lenticular. The rounded to sub-rounded limestone nodules floating in micrite matrix range from 20–25 cm and dark grayish to black chert nodules are 8–10 cm in diameter. This unit is also highly fractured.

Upper massive nodular limestone with chert nodules

This unit is 22.7 m thick. The limestone is hard massive, yellowish to grayish on weathered surface and yellow to light grayish on fresh surface and the size of limestone nodules ranges from 16 to 25 cm in diameter (Fig. 4d). The chert nodules are well concentrated in this unit and size of the chert nodules is 5–15 cm. The ratio of micrite matrix increases upward in this unit.

The well-developed crystals of replaced calcite are also found in the upper unit (Fig. 4e). The size of the foraminifera increases towards the top of the unit. At the KTS, the lower part of Sakesar Limestone is not exposed (Fig. 3). The upper part of the middle unit is exposed while upper contact with the Chorgali Formation is conformable in this section. Here, the thickness of the Sakesar Limestone is 19 m. This section is similar to uppermost unit of the NGS with well-developed vertical open fractures (Fig. 4f). At the NGS, the formation has both gradational contacts with the underlying Nammal Formation and overlying Chorgali Formation but at the KTS, the lower contact is concealed and upper contact with Chorgali Formation is gradational (Fig. 4g, h).

Petrographic analysis

The details of main petrographic characteristics like type and percentage of grains, amount of carbonate matrix, spar and visually estimated porosity are calculated. Subsequently, the petrographic data are used to describe the microfacies. The microfacies leads to the interpretation of the depositional environments of the Sakesar Limestone that in turn helpful

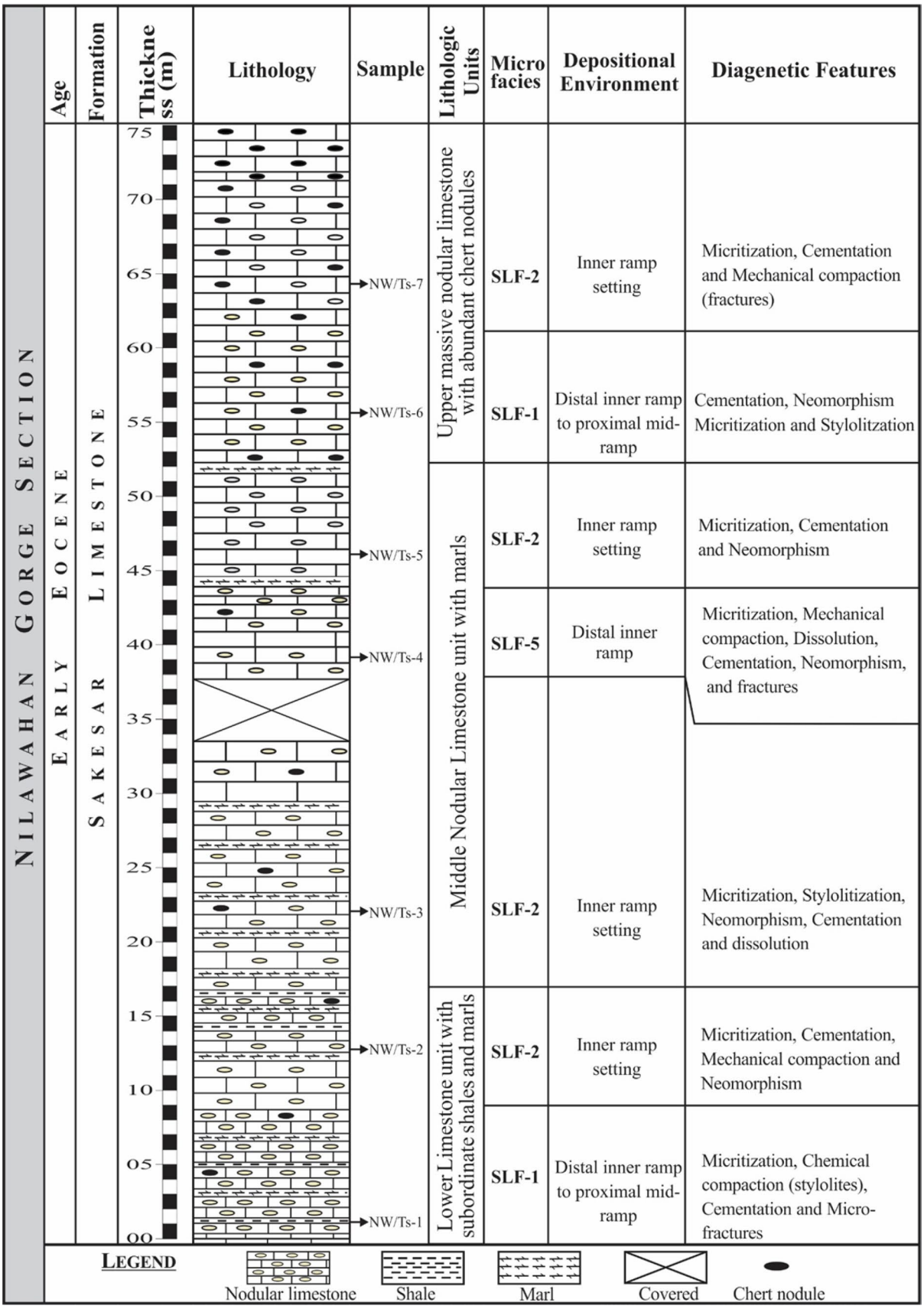

Fig. 2 The vertical distribution of microfacies, depositional environment and diagenetic processes of the Sakesar Limestone at the NGS, Central Salt Range

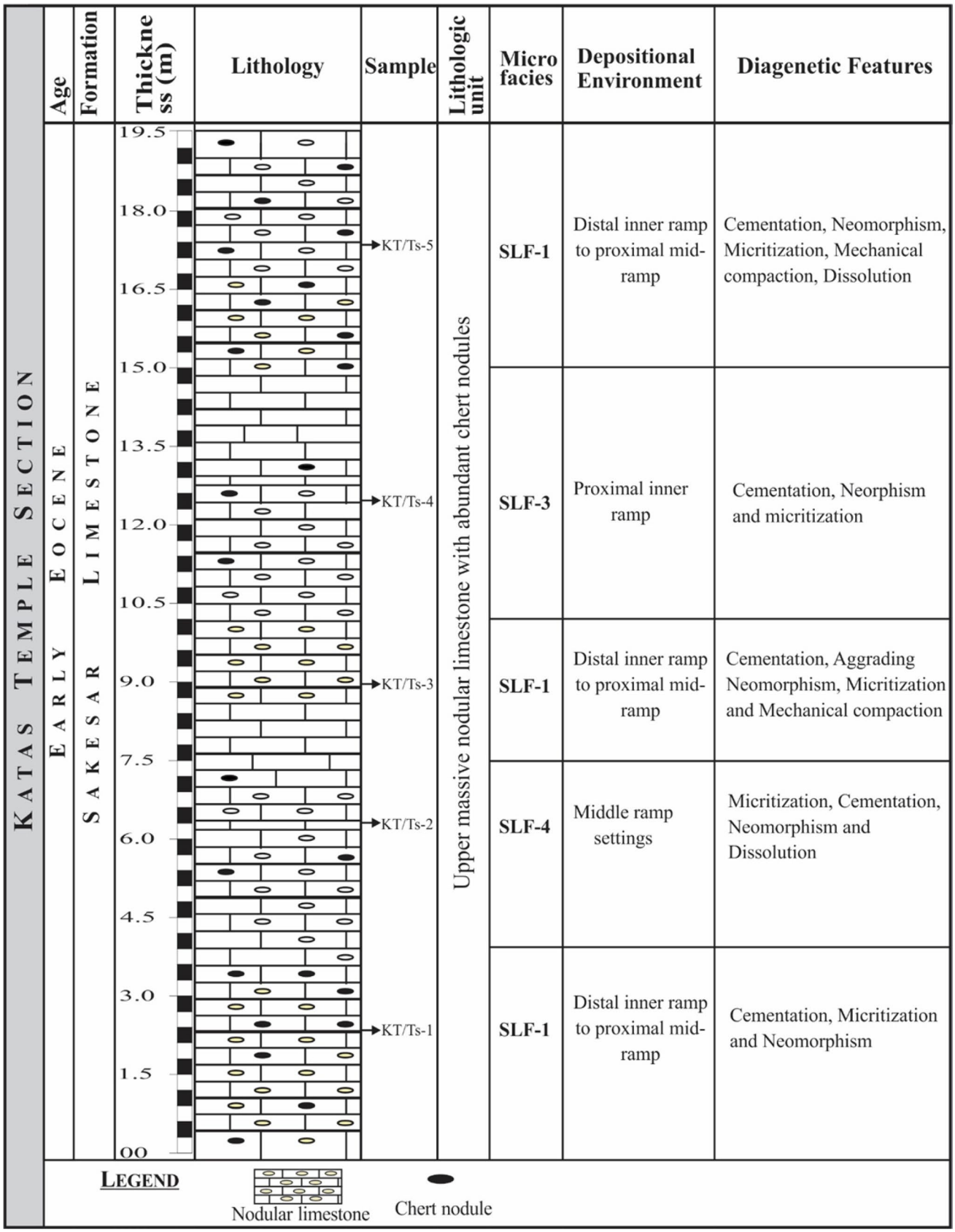

Fig. 3 The vertical distribution of microfacies, depositional environment and diagenetic processes of the Sakesar Limestone at the KTS, Eastern Salt Range

to propose a depositional model for the Sakesar Limestone. The main aim of carbonate petrography is to classify the limestone. The important petrographic characteristics such as type of allochems, matrix, cement (spar) and type of pores are recognized in the Sakesar Limestone (Table 1).

The skeletal allochems (bioclasts) and orthochems (micrite and sparite) are recognized in the Sakesar Limestone. The petrographic characteristic features of the Sakesar Limestone in the NGS and KTS are mostly represented by skeletal grains in a micrite matrix where some samples contain sparse sparite. Some samples from NGS also contain dolomite. The skeletal grains are composed of larger benthonic foraminifera, some smaller benthonic foraminifera, green algae, broken or whole gastropods, echinoids and some ghost fossils. The larger benthonic foraminifera comprise species of Assilina, Nummulites, Lockhartia, Alveolina, Miliolid and Textularia, etc. The two types of sparite are recognized in the Sakesar Limestone, i.e., sparry calcite and Ferroan sparite (iron stained). Petrographically, the Sakesar Limestone is classified as micritic limestone.

Microfacies of the Sakesar Limestone

The microfacies of the Sakesar Limestone have been identified from bottom to top in the NGS and KTS, respectively. The Sakesar Limestone is composed of skeletal microfacies only. Following Dunham classification (1962), the two major carbonate microfacies recognized within the Sakesar Limestone are wackestone and packstone. These two main microfacies contain skeletal grains in variable proportions. Considering their distribution within the wackestone and packstone, the following microfacies have been established.

Benthonic Foraminiferal wackestone (SLF-1) The SLF-1 microfacies is represented by thin sections NW/Ts-1 and NW/Ts-6 from the NGS and KT/Ts-1, KT/Ts-3 and KT/Ts-5 of KTS which is recognized by wackestone depositional texture (Fig. 5a–f). The dominant constituents of this microfacies are micrite matrix and skeletal allochems. The micrite matrix ranges from 51 to 67.32% with an average of 61.50% (Table 1). The biogenic contents are moderately preserved. The skeletal grains are ranging from 13 to 32% with an average of 21.29%. The skeletal allochems are dominantly composed of benthonic foraminifera. The assemblage benthonic foraminifera include *Nummulites* sp., *Assilina* sp., *Alveolina* sp., *Lockhartia* sp. and miliolids. The minor skeletal grains are of algae, planktonic foraminifera, gastropods, broken shell fragments and few ghost. The algae comprised dasyclad green algae. The sparry calcite is ranging from 5.5 to 19% with an average of 14.2% and ferroan sparite ranges from 03 to 06% with an average of 2.13%. The porosity varies from 0.35 to 1.23% with an average of 0.736% (Table 1).

Interpretation

The *Nummulites* sp. in association with *Assilina* sp. represent deeper inner to middle ramp depositional conditions (Buxton and Pedley 1989; Racey 2001; Beavington-Penney and Racey 2004; Vaziri-Moghaddam et al. 2006; Adabi et al. 2008; Payros et al. 2010). The *Alveolina* sp. and miliolids represent shallow warm water conditions of inner ramp setting (Gilham and Bristow 1998; Racey 2001; Beavington-Penney and Racey 2004). The co-occurrences of *Nummulites* and *Alveolina* are possibly imitating the mixing of inner ramp to middle ramp environments (Gilham and Bristow 1998; Hohenegger et al. 1999; Racey 2001; Beavington-Penney and Racey 2004). However, the presence of abundant micrite matrix in combination of various skeletal allochems belonging to the benthonic foraminifera indicate that the SLF-1 microfacies was deposited in the distal inner ramp to proximal mid-ramp depositional setting with some restricted lagoonal conditions.

Foraminiferal-Algal wackestone–packstone (SLF-2) The SLF-2 microfacies is recognized by wackestone to packstone depositional texture and is represented by thin sections NW/Ts-(2, 3, 5 and 7) from NGS (Fig. 6a–c). The dominant constituents of this microfacies are micrite matrix and skeletal allochems. The micrite matrix varies from 47 to 54.37% with an average of 49.47%. The skeletal allochems are 35–41% with an average of 37.8% (Table 1). The allochems majorly include benthonic foraminifera, i.e., *Nummilties* sp., *Assilina* sp., *Alveolina* sp., *Lokhartia* sp, and miliolids followed by dasycladale green algae. The rare allochems include broken shell fragments and some ghost. The sparry calcite varies between 06 and 16% with an average of 8.09% and ferroan calcite ranges from 3 to 5% with an average of 3.1% (Table 1).

Interpretation

The *Nummulites* indicate wide spectrum of open marine conditions of inner ramp to middle ramp whereas smaller lenticular *Nummulites* are widely distributed in inner ramp setting in association with alveolinids (Loucks et al. 1998; Racey 2001; Beavington-Penney and Racey 2004; Vaziri-Moghaddam et al. 2006; Payros et al. 2010; Mehr and Adabi 2014) and most suitable conditions prevail in inner ramp photic zone (< 20 m) with abundant food supply and low to moderate water turbulence (Hallock 1985; Racey 1994, 2001; Adabi et al. 2008). The association of *Alveolina* sp., *Lockhartia* sp, and miliolids followed by dasycladale green algae indicates inner ramp setting of low water turbulence and restricted conditions (Racey 1994; Beavington-Penney et al. 2006; Adabi et al. 2008). However, based on dominant matrix-supported rock fabric,

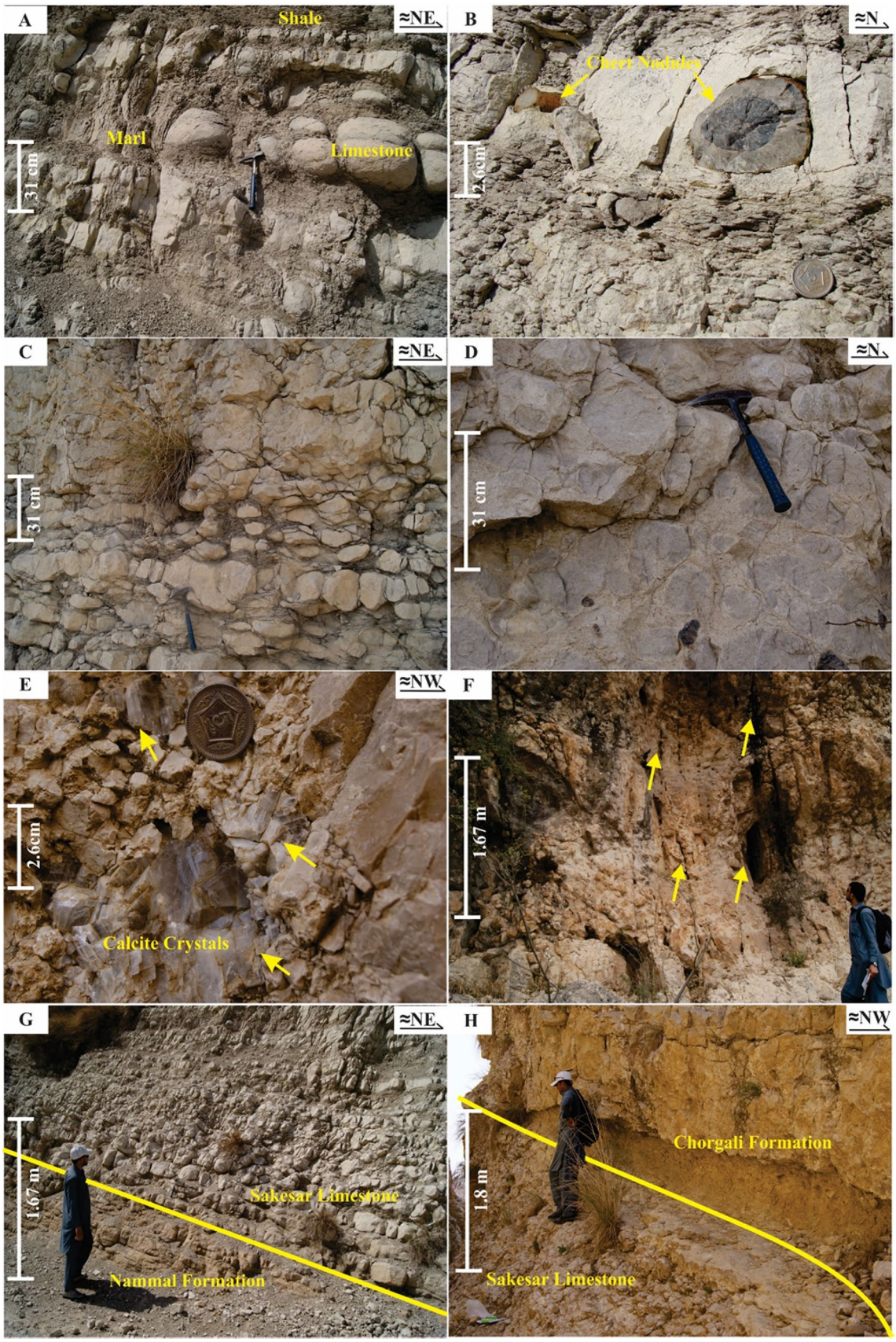
A
Shale
≈NE
Marl
Limestone
31 cm
B
≈N
Chert Nodules
2.6cm
C
≈NE
31 cm
D
≈N
31 cm
E
≈NW
2.6cm
Calcite Crystals
F
1.67 m
G
≈NE
1.67 m
Sakesar Limestone
Nammal Formation
H
≈NW
Chorgali Formation
1.8 m
Sakesar Limestone

◂**Fig. 4** Field photographs of the Sakesar Limestone. **a** Lower unit of Sakesar Limestone, NGS. **b** Chert nodules in lower unit, NGS. **c** Middle nodular limestone unit of Sakesar Limestone, NGS. **d** Upper cherty limestone unit, NGS. **e** Calcite crystals in the upper unit of Sakesar Limestone, NGS. **f** Vertical open fractures, Sakesar Limestone, KTS. **g** Lower contact of the Sakesar Limestone with the Nammal Formation, NGS. **h** Upper contact of the Sakesar Limestone with the Chorgali Formation, NGS

the moderate to low diversity of foraminifera, presence of restricted marine fauna suggest that the SLF-2 microfacies was deposited in inner ramp lagoonal settings.

Miliolidal-Algal wackestone–packstone (SLF-3) The SLF-3 microfacies is characterized by wackestone–packstone depositional texture and is represented by thin section KT/Ts-4 of KTS (Fig. 7a–c). The preservation of biogenic contents is moderate to poor. The skeletal grains vary between 15 and 45% with an average of 32.5% (Table 1). The predominant skeletal allochems are of miliolids followed by algae (dasycladales). The other rare allochems include gastropods, planktons, broken shell fragments and some ghost. Some micritized skeletal allochems are difficult to identify. The micrite matrix is ranging from 45 to 67% with an average of 54%. The sparry calcite is ranging from 5 to 30% with an average of 13.5% (Table 1). The fracture filled calcite cement is well preserved.

Interpretation

The miliolids favor calm and quite shallow-water conditions and their great abundance suggests nutrient rich and a lagoonal marine condition of inner ramp (Racey 1994; Geel 2000; Beavington-Penney et al. 2006; Adabi et al. 2008; Swei and Tucker 2012; Mehr and Adabi 2014). The low diversity of associated foraminifera and the presence of abundant miliolids are good indication of saline to hypersaline shallow marine conditions (Mehr and Adabi 2014). The dasycladal green algae favors upper euphotic zone of shallow warm-water which is predominantly low energy and confined to marine lagoonal conditions of inner ramp (Wray 1977; Berger and Kaever 1992; Beavington-Penney et al. 2006; Granier 2012). In calm and quiet environments, dasycladale algae cannot be assumed more than 20% of the coarse grains and in such conditions, this is because of micritization and degree of mineralization (Macintyre and Reid 1995). However, the association and abundance of miliolid foraminifera and green algae with the predominant contents of micrite matrix suggest that the SLF-3 microfacies was deposited in shallow water lagoonal conditions of proximal inner ramp settings (Vaziri-Moghaddam et al. 2006; Brandano et al. 2009).

Nummulitic-Assilina packstone (SLF-4) The SLF-4 microfacies is represented by thin section KT/Ts-2 of the KTS (Fig. 8a–f). The predominant constituents of this microfacies are skeletal allochems and micrite mud. The visual estimation of allochemical constituents to matrix is 5:5. The skeletal allochems are 45–75% with an average of 51% (Table 1). The biogenic contents are well preserved. The benthonic foraminifera are the predominant allochems that includes *Nummulitic* sp., followed by *Assilina* sp. The other skeletal allochems including *Alveolina* sp., miliolids, some planktons, broken shell fragments and highly micritized skeletal allochems represent ghost. The micrite varies between 24 and 45% with an average of 40.46%. The average sparry calcite is 8% and the porosity varies between 0.45 and 1.23% with 0.54% average porosity within this microfacies (Table 1).

Interpretation

The *Nummulites* are reported from different parts of the world that predominantly represent middle ramp environment and when associated with *Assilina* sp. then represent a relatively deeper environment (Racey 1994; Anketell and Mriheel 2000; Racey 2001;Vaziri-Moghaddam et al. 2006; Adabi et al. 2008; Payros et al. 2010; Mehr and Adabi 2014). The Alveolina represent warm water condition (Hohenegger et al. 1999). The miliolidal species essentially are of low turbulence waters and a soft substrate whereas their large abundance indicates restricted lagoonal conditions (Geel 2000; Vaziri-Moghaddam et al. 2006; Brandano et al. 2009). However, apparently the high diversity of *Nummulites* sp. and *Assilina* sp. and micritic matrix indicate that SLF-4 is deposited in low-energy conditions of middle ramp settings.

Alveolina-Algal packstone (SLF-5) The SLF-5 microfacies is represented by thin section NW/Ts-4 of the NGS and is characterized by bioclastic packstone depositional texture (Fig. 9a–c). This microfacies is grain supported but contains micritic mud. The biogenic contents of the microfacies are well preserved. The allochemical constituents are predominantly skeletal that varies between 46 and 72% with an average of 58% (Table 1). The skeletal allochems are well preserved. The predominant skeletal allochems are of *Alveolina* sp. followed by algae. The other skeletal allochems include *Lockhartia* sp., *Assilina* sp., broken shell fragments and few ghost fossils. The micrite matrix varies between 15 and 49% with an average of 28%. The average sparry calcite is 8% and ferroan calcite is 4%. The porosity is ranging from 1 to 6% with an average of 1.4% (Table 1). This microfacies is highly fractured and yields fracture porosity (Fig. 9a, c).

Table 1 The visually estimated petrographical constituents (allochems, orthochems, flora and fauna) of the Sakesar Limestone

Sample	Skeletal allochems (%)	Orthochems			Porosity (%)	Foraminifers						Gastropods (%)	Algae (%)	Bioclastic fragments (%)	Ghost (%)
		Sparite cement		Matrix (%)		Nummulities sp. (%)	Assilina sp. (%)	Alveolina sp. (%)	Lokhartia sp. (%)	Miliolid (%)	Plankonic Forams (%)				
		Sparry (%)	Ferroan (%)												
NW/Ts-7	38	5.45	4.55	51	1.03	06	03	07	05	02	01	1.5	1.05	01	01
01	29.5	17	–	53	0.54	10	07	3.5	03	01	0.5	–	02	–	–
NW/Ts-5	39	16	–	44.33	0.67	08	6.5	5.5	02	1.5	–	01	12.5	02	–
NW/Ts-4	58	08	04	28	02	01	03	29	05	01	–	1.5	12	01	2.5
NW/Ts-3	41	06	3.95	47	2.05	9.5	11	4.5	09	0.5	1.5	0.5	–	1.5	–
NW/Ts-2	36	07	04	52	01	6.5	05	6.5	3.5	–	0.5	–	9.5	2.5	1.5
NW/Ts-1	20	11	03	64.77	1.23	05	03	2.5	03	0.5	–	0.5	02	1.5	02
KT/Ts-5	13	19	06	60.12	1.88	3.5	01	02	2.5	0.5	–	–	1.5	–	0.5
KT/Ts-4	32.5	9.5	04	54	0.63	–	–	–	–	15.5	02	1.5	11	01	1.5
KT/Ts-3	22	14	1.65	62	0.35	06	2.5	03	03	01	0.5	0.5	2.5	–	3
KT/Ts-2	51	08	–	40.46	0.54	14.5	12	08	6.5	03	1.5	–	03	01	1.5
KT/Ts-1	22	10	–	67.32	0.68	7.5	1.5	3.5	3.5	1.5	–	–	02	02	1.5

Interpretation

The *Alveolina* sp. represents shallow warm water conditions with a depth range 5-80 m (Buxton and Pedley 1989; Hohenegger et al. 1999; Beavington-Penney and Racey 2004) found on all substrates in nummulitic-back bank areas of shallow-water often have symbiont bearing algae (Geel 2000). The dasycladale green algae presumably found in low energy, warm waters and protected lagoonal regimes (Wray 1977; Berger and Kaever 1992; Beavington-Penney et al. 2006; Adabi et al. 2008). However, predominant association of *Alveolina* sp., dasycladale green algae and micrite matrix are characteristic constituents of this microfacies that suggest low-energy distal inner ramp with restricted lagoonal conditions (Scheibner et al. 2007; Höntzsch et al. 2011). The *Lockhartia* sp. indicates inner to middle ramp setting (Racey 1994). Hence, SLF-5 microfacies reflects shallow water, low energy conditions in distal inner ramp settings.

Diagenesis of the Sakesar Limestone

The diagenetic study of the Sakesar Limestone comprised following major diagenetic processes examined on microscopic scale and some on macroscopic scale. Such study is utmost important in case of the Sakesar Limestone because the diagenetic processes may either erect barriers to the fluid flow or it may provide selective passageways for the migration of fluids and, hence, the diagenetic processes have influential control on the subsurface fluids composition and on subsurface porosity distribution. Thus, there are many compelling applied aspects to diagenetic studies of the Sakesar Limestone. Petrographic studies showed that several diagenetic processes including micritization, compaction, neomorphism, dissolution, cementation, fracturing and vein formation had affected the Sakesar Limestone. The limestone nodularity and chert nodules (silicification) are diagenetic processes that have been noted on macroscopic level along with vertical fractures. All diagenetic processes are summarized in Table 2. Likewise, all the diagenetic features of each sample of NGS and KTS are shown in Figs. 2 and 3, respectively.

Micritization

Micritization or degrading recrystallization causes the conversion and destruction of skeletal and non- skeletal grains into structureless and homogeneous masses of translucent to opaque massive micrite (Khalifa 2005; Abu-El Ghar et al. 2015) that occurs at the sediment–water interface (Adams and MacKenzie 1998) under low-energy conditions (Tucker and Wright 1990; Flügel 2010). In the Sakesar Limestone, the most important and the earliest diagenetic process is micritization (Adams and MacKenzie 1998) that takes place in

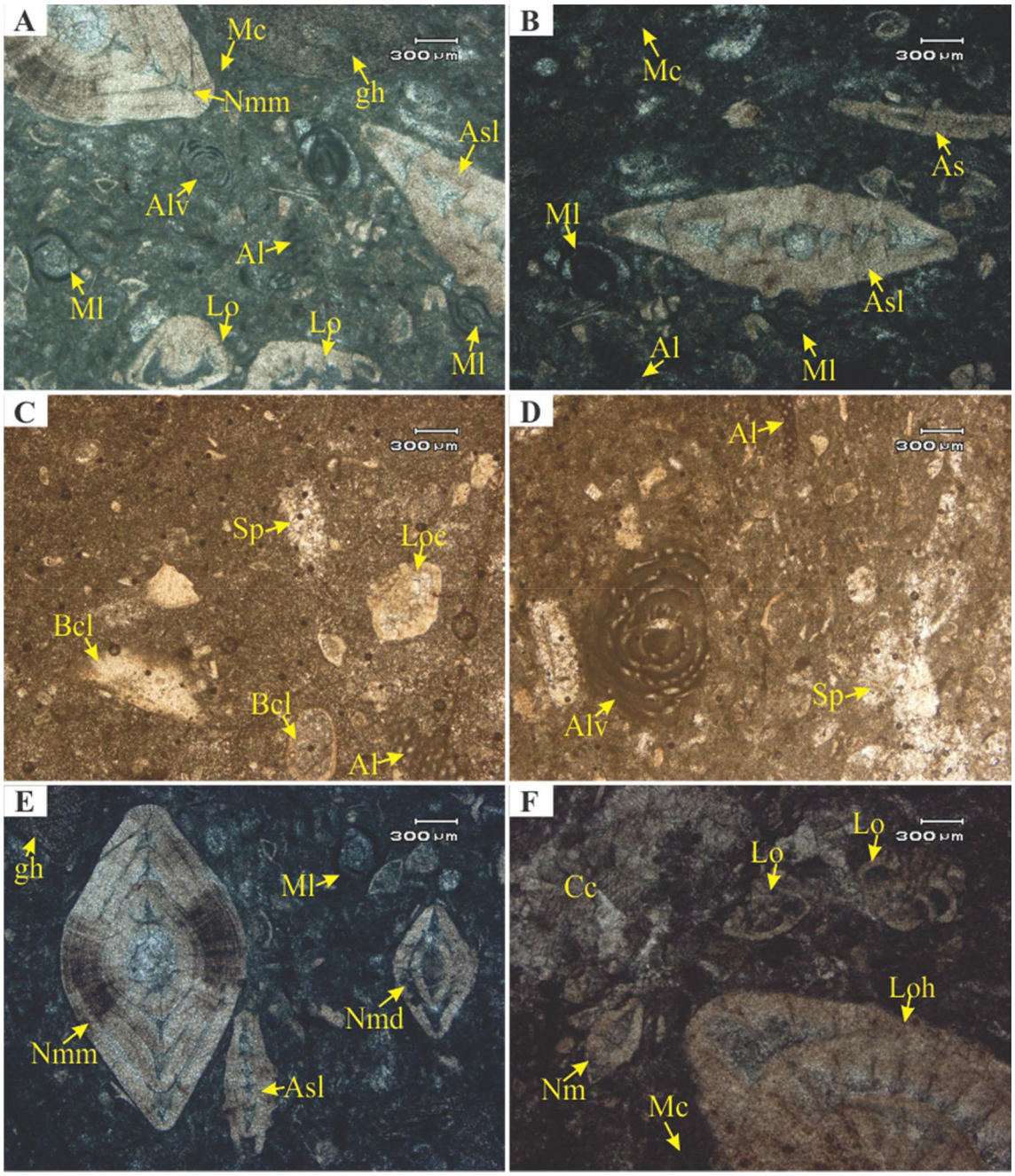

Fig. 5 Benthonic Foraminiferal wackestone (SLF-1): the skeletal allochems of the microfacies include larger benthonic foraminifera, i.e., *Nummulites mamillatus* (Nmm in **a**, **e**), *Nummulites djodjokartae* (Nmd in **e**), *Nummulites sp*. (Nm in **f**), algae (Al in **a**–**d**), miliolids (Ml in **a**, **b**, **e**), *Assilina leymerie* (Asl in **a**, **b**, **e**), *Assilina* sp. (As in **b**), *Lockhartia* sp. (Lo in **a**, **c**, **f**), *Lockhartia haimei* (Loh in **f**), *Alveolina globula* (Alv in **a**, **d**), broken and altered allochems (Bcl in **c**) and ghost (gh in **a**, **e**) scattered in micrite matrix (Mc in **a**, **b**, **f**). The sparry calcite is represented by Sp (in **c**, **d**) and crystalline calcite is represented by Cc (in **f**). Photomicrographs are from samples NW/Ts-6 (**a**, **b**, **e**, **f**), KT/Ts-1 (**c**) and KT/Ts 3 (**d**)

two phases, i.e., (a) bioclast micritization is common where the chambers of bioclasts are occupied by micrite (Fig. 10a; Bathurst 1975; Vincent et al. 2007) and (b) the micritic envelopes that mostly develop around the bioclasts and other grains (Fig. 10b) represented by the repetitive activity of endolithic algae on the carbonate grains surfaces (Vincent 2001; Carols 2002; Vincent et al. 2007; Brigaud et al. 2009).

The micritization in the Sakesar Limestone is noted in almost all samples of both NGS and KTS (Table 2; Figs. 2, 3). The studied samples are highly micritized and affected

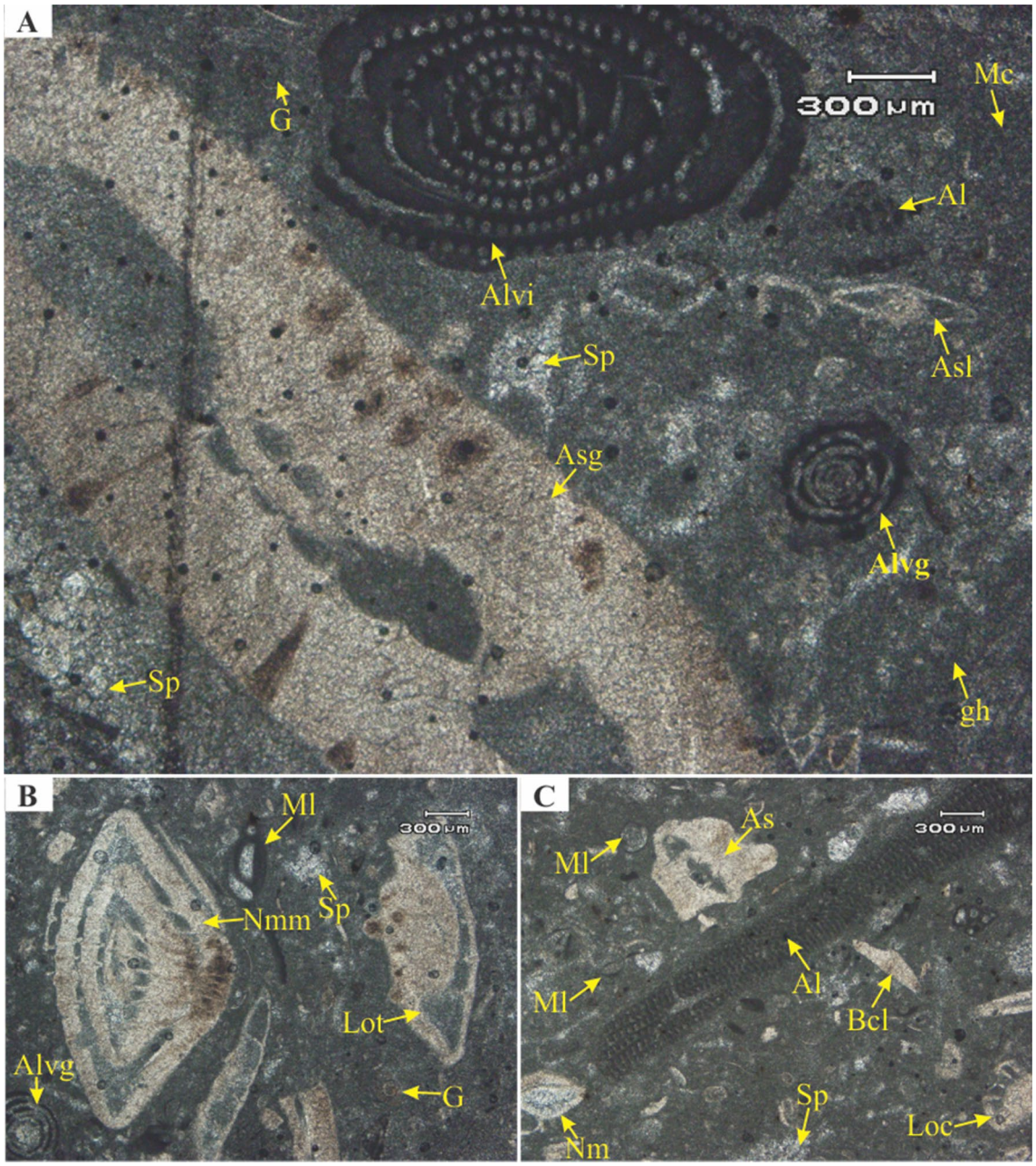

Fig. 6 Foraminiferal-Algal wackestone–packstone (SLF-2): The skeletal allochems of this microfacies includes foraminifera and algae, i.e., *Alveolina indicatrix* (Alvi in **a**), *Alveolina globosa*. (Alvg in **a**, **b**), *Assilina granulosa* (Asg in **a**), *Assilina laminosa* (Asl in **a**), *Assilina* sp. (As in **c**), *Nummulites mammilatus* (Nmm in **b**), *Nummulites* sp. (Nm in **c**), *Lockhartia conditi* (Loc in **c**), *Lockhartia tipperi* (Lot in **b**), milliolids (Ml in **b**, **c**), gastropod (G in **a**, **b**), Dasycladacean green algae (Al in **c**), broken fragment (Bcl in **c**) which is scattered in micrite matrix (Mc in **a**). The sparry calcite is represented by Sp (in **a**–**c**). Photomicrographs are from samples NW/Ts-5 (**a**, **b**) and NW/Ts-7 (**c**)

the skeletal grains as well as non-skeletal particles. It forms thin micrite envelopes around certain grains and in others led to destruction of most parts with patches of micrite present (Fig. 10a). The micritization is the earliest most event in the Sakesar Limestone as well as of paragenetic sequence (Vincent et al. 2007). This extensive micritization in the Sakesar Limestone proposes that this process and the resulting deterioration structures of bioclasts are the evidences of intense microbial activity on the carbonate grain surfaces in the Sakesar Limestone.

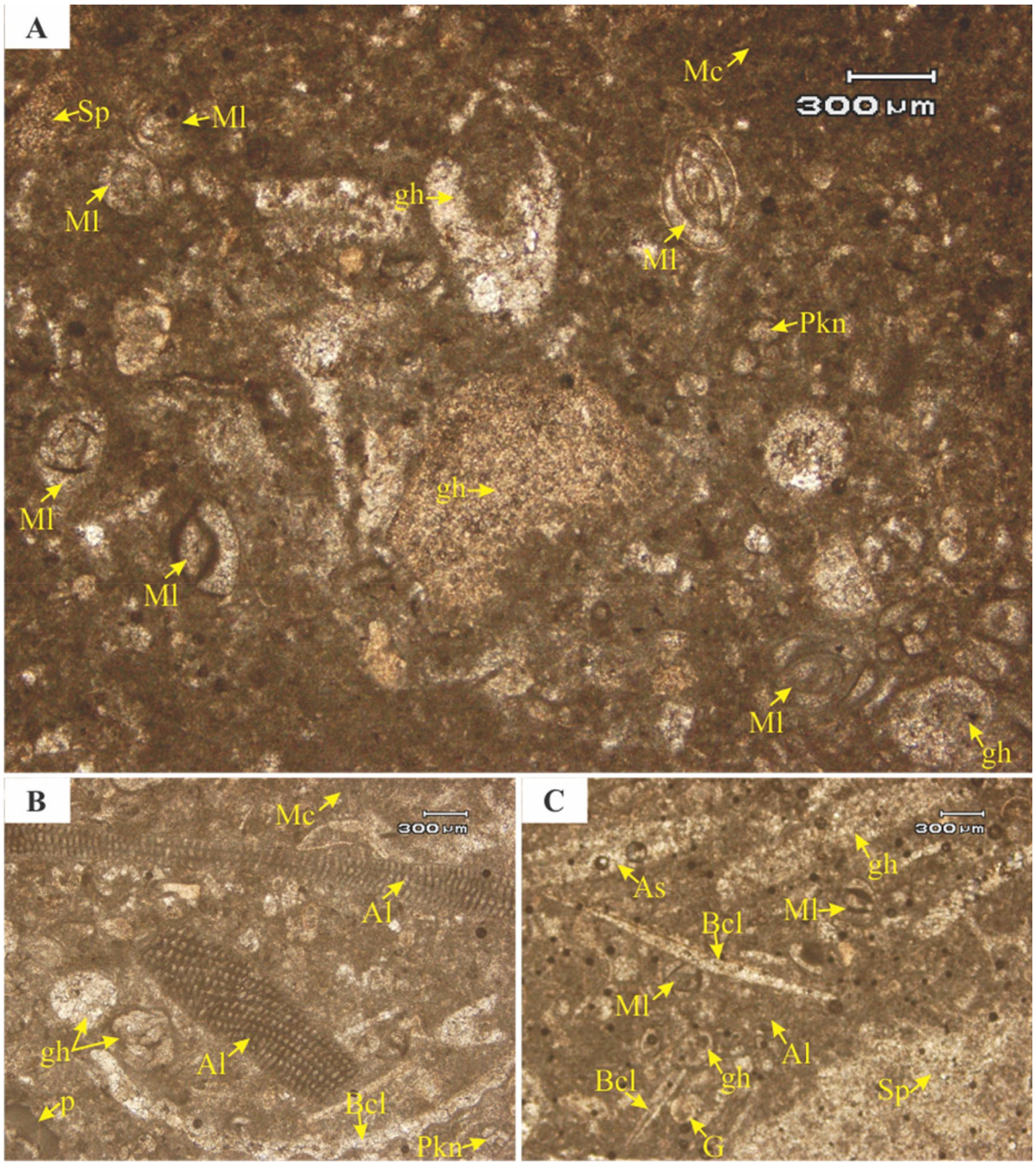

Fig. 7 Miliolidal-Algal wackestone–packstone (SLF-3): the skeletal allochems of the microfacies include: miliolid (Ml in **a**, **c**), Dasyclade green algae (Al in **b**, **c**), planktonic foraminifera (Pkn in **a**, **b**), gastropod (G in **c**), broken shell fragments (Bcl in **b**, **c**) and ghost (gh in **a**–**c**) embedded in micrite matrix (Mc in **a**, **b**). The dissolution porosity (p in **b**) and sparry calcite (Sp in **a**, **c**) are shown. Photomicrographs are from sample KT/Ts-4 (**a**–**c**)

Cementation

The cementation is widely distributed diagenetic event in the Sakesar Limestone (Fig. 10c–f). The identified cement types and cement fabrics in the Sakesar Limestone include isopachous fibrous, blocky calcite cement, granular mosaic and poikilotopic cement.

Isopachous fibrous cement This is the first-generation cement that formed around the bioclasts and is noted in sample KT/Ts-3 of wackestone–packstone. It displays isopachous fibrous and bladed shapes and shaped around grain rims or micrite envelops (Fig. 10c). This cement is typically formed in the marine phreatic environment probably representing synsedimentary cementation (Melim

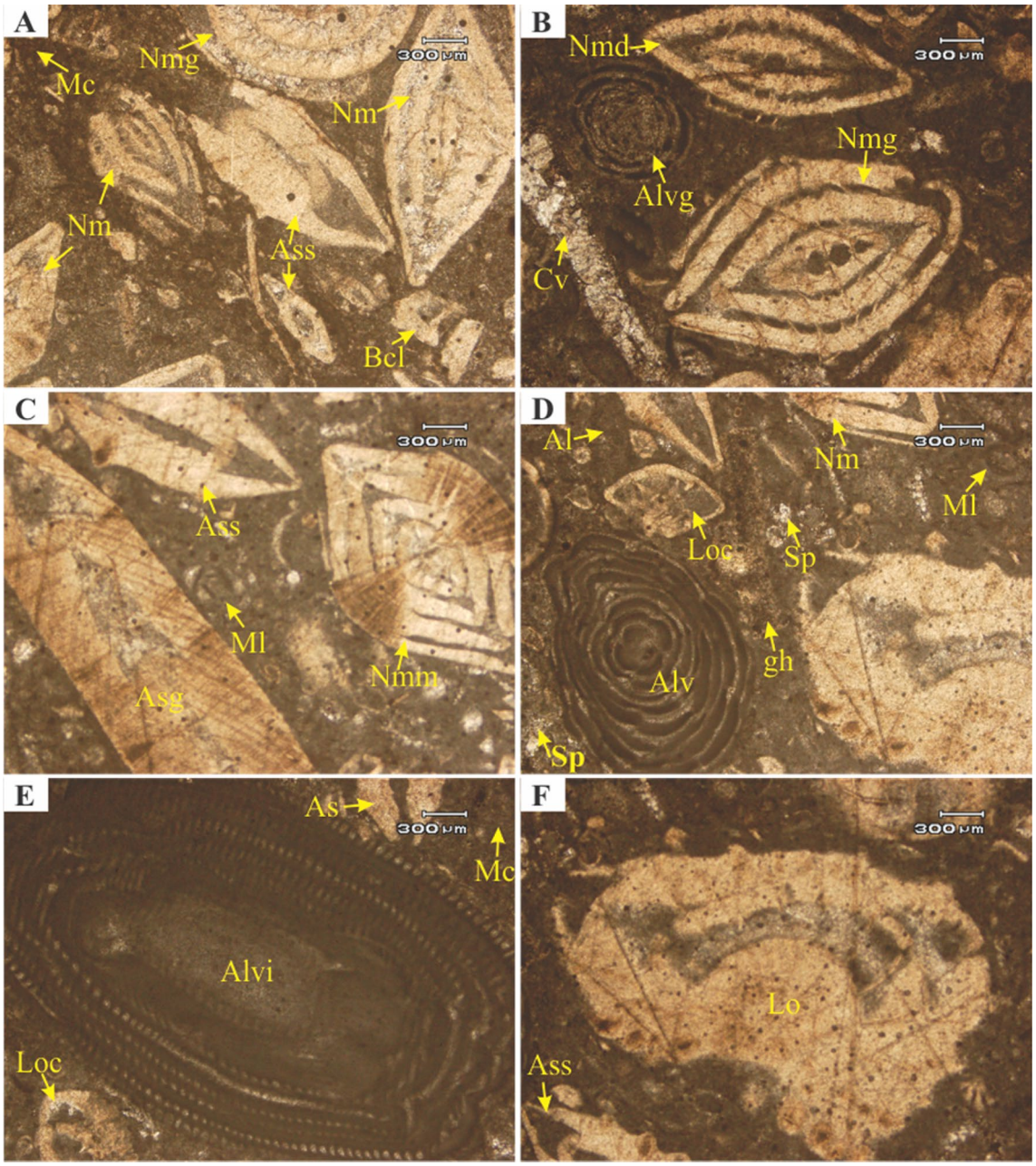

Fig. 8 Nummulitic-Assilina packstone (SLF-4): the skeletal allochems of this microfacies include the larger benthonic foraminifera; (Nmg in **a**, **b**), *Nummulites mammilatus* (Nmm in **c**), *Nummulites djodjokartae* (Nmd in **b**) *Nummulites globulus* (Nmg in **b**), *Nummulites* sp. (Nm in **a**, **d**), *Assilina subspinosa* (Ass in **a**, **c** and **f**), *Assilina granulosa* (Asg in **c**), *Assilina* sp. (As in **e**), *Alveolina globosa* (Alvg in **b**), *Alveolina indicatrix* (Alvi in **e**), *Alveolina* sp. (Alv in **d**), *Lockhartia conditi* (Loc in **d**, **e**), *Lockhartia* sp. (Lo in **f**), milliolid (Ml in **c**, **d**), ghost (gh in **d**) and broken shell fragments (Bcl in **a**) embedded in micrite matrix (Mc in **a**, **e**). The sparry calcite cement (Sp in **d**) and calcite filled vein (Cv in **b**) are also present. Photomicrographs are from sample KT/Ts-2 (**a**–**f**)

et al. 2002; Vincent et al. 2007) that reflects Mg carbonate saturation state where its formation is favored by low sedimentation rate (Ehrenberg et al. 2012). The isopachous fibrous cement is rarely developed rimming the skeletal allochems and usually have Mg-calcitic in composition (Tucker and Wright 1990; Harris et al. 1997; Khalifa 2005).

Blocky calcite cement The blocky cement is noted in samples NW/Ts-3, NW/Ts-4, NW/Ts-6, KT/Ts-4 and KT/Ts-6. There are two stages of blocky calcite cement in the Sake-

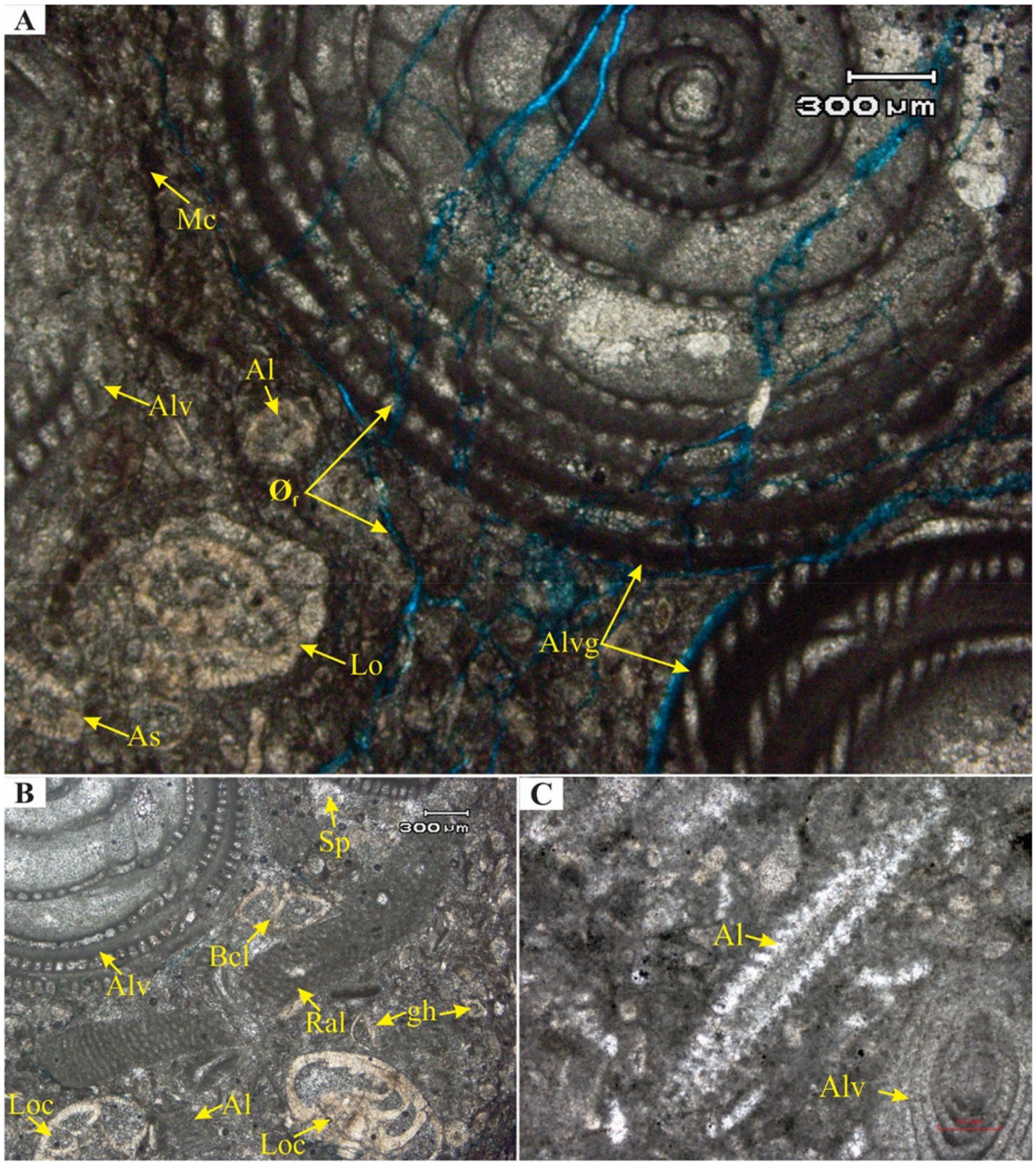

Fig. 9 Alveolina-Algal packstone (SLF-5): The allochems of the microfacies include *Alveolina globula* (Alvg in **a**), *Alveolina* sp. (Alv in **a**–**c**), *Lokhartia conditi* (Loc in **b**), *Lockhartia* sp. (Lo in **a**), *Assilina* sp. (As in **a**), Dasyclad green algae (Al in **a**–**c**), broken shell fragments (Bcl in **b**), and ghost (gh in **b**) embedded in micrite matrix (Mc in **a**). Fracture porosity ($Ø_f$ in **a**) and sparry calcite cement (Sp in **b**). Photomicrographs are from sample NW/Ts-4 (**a**–**c**)

sar Limestone: a) this type of blocky cement is well developed and occupying the intergranular, primary intra-skeletal pores of perforate foraminifera and also in the molds of the early dissolve grains (Fig. 10d). This type of blocky calcite cement is developed during the meteoric-phreatic diagenesis (Khalifa et al. 2009; Abu-El Ghar et al. 2015). In meteoric-phreatic zone, the pores are predominantly filled with water where cementation is more even with crystal growth that yields larger crystal size of blocky calcite cement (Tucker and Wright 1990). This cement was also noted in the development of aggrading neomorphism, b) the second type of blocky cement is found within the fractures that partially or entirely filled the fractures (Fig. 10e). This stage corresponds to only one generation of blocky cement in the Sakesar Limestone which is identified by undulatory extinction and is the diagnostic of burial realm (Andre 2003; Vincent

Table 2 Diagenetic processes identified in the Sakesar Limestone at Nilawahan Gorge (NW/Ts) and Katas Temple (KT/Ts) sections

Sample #	Micritization	Cementation	Dissolution	Neomorphism	Limestone nodularity	Silicification	Mechanical compaction	Chemical compaction	Fractures	
									Micro	Macro
NW/Ts-7	✓	–	✓	–	Macro scale	Macro scale	–	✓	✓	Macro scale
NW/Ts-6	✓	✓	–	✓			–	✓	–	
NW/Ts-5	✓	✓	–	✓			–	–	–	
NW/Ts-4	✓	✓	✓	✓			✓	✓	✓	
NW/Ts-3	✓	✓	✓	✓			–	✓	✓	
NW/Ts-2	✓	✓	–	✓			✓	–	–	
NW/Ts-1	✓	✓	–	–			–	✓	✓	
KT/Ts-5	✓	✓	✓	✓			✓	–	✓	
KT/Ts-4	✓	✓	–	✓			–	–	–	
KT/Ts-3	✓	✓	–	✓			✓	–	✓	
KT/Ts-2	✓	✓	✓	✓				–	–	
KT/Ts-1	✓	✓	–	✓				–	–	

et al. 2007). Both phases of blocky calcite cement are compositionally non-ferroan low magnesium calcite (Vincent et al. 2007; Brigaud et al. 2009).

The chronological order of these two stages of blocky cements cannot be established just from diagenetic microstratigraphy but, however, mesogenetic history of sediment might be inferred to their distribution (Vincent et al. 2007) in the Sakesar Limestone. In terms of paragenetic activity of above-mentioned stages of blocky cements, the stage-a is formed earlier than the stage-b as evidenced from the cross-cutting relation of these two stages.

Poikilotopic cement This cement was noted in sample KT/Ts-4 of the Sakesar Limestone that consists of larger crystal(s) that contain smaller bioclast grains (Fig. 10d; Flügel 2010; Mahboubi et al. 2010). It is scarcely noted cement type in the studied samples. It is formed from calcium carbonate supersaturated pore fluids that have low calcite crystal nucleation rate and growth rate (Mahboubi et al. 2010). When meteoric-phreatic zone freshwater mimics downward into burial zone, poikilotopic cement forms and represents the burial diagenetic environment (Nader 2017).

Granular mosaic cement This is uncommon cement found in the Sakesar Limestone and was noted in sample NW/Ts-2 of wackestone microfacies. This is the pore filling cement between skeletal and non-skeletal grains that developed as subhedral crystals (Fig. 10f; Mahboubi et al. 2010). This cement represents meteoric-phreatic environment (Abu-El Ghar et al. 2015) and usually associated with green algae and miliolid skeletal allochems in the Sakesar Limestone.

Dissolution

This process has affected most of the Sakesar Limestone in the studied sections. However, the obvious dissolution features in the Sakesar Limestone were noted in samples NW/Ts-3, NW/Ts-4, KT/Ts-2 and KT/Ts-5. The dissolution identified in the Sakesar Limestone contributes three stages: (a) early dissolution in the marine meteoric stage where most of the metastable skeletal grains and intergranular cements are dissolved when the pores are undersaturated with respect to carbonate minerals. These pores either constitute biomoldic porosity (Fig. 11a) or filled by blocky calcite cement. (b) Intergranular microcrystalline cement dissolution where cements are dissolved and micropores developed (Fig. 11b). (c) The selective dissolution of blocky calcite cement in the calcite filled veins is noted in sample KT/Ts-5 (Fig. 11c). This stage demonstrates that first fractures developed in the burial environment where fractures are evolved as veins by later filling of blocky calcite cement and then further burial took place and selective dissolution of blocky calcite cement has taken place during uplifting (Fig. 11c). The later

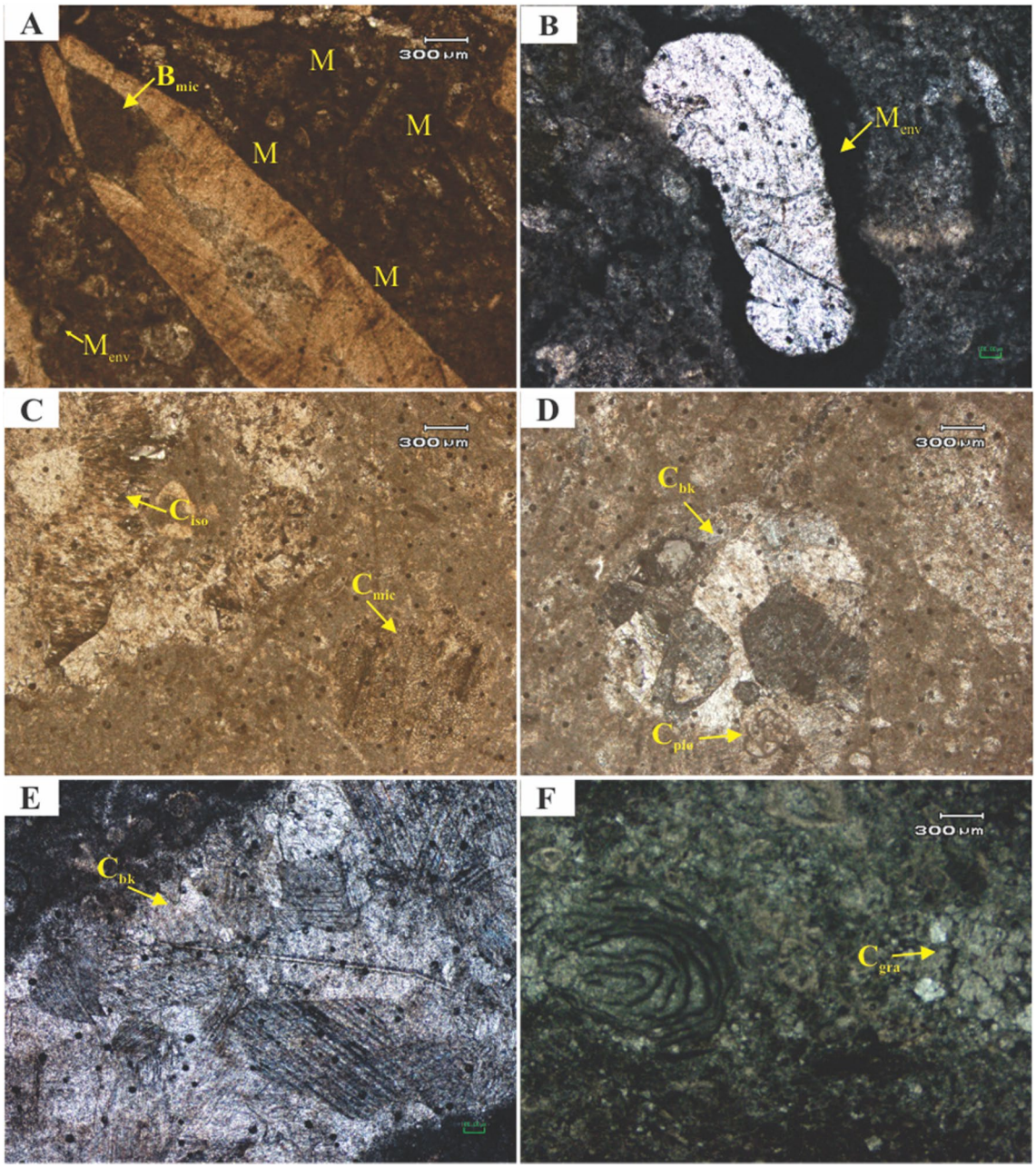

Fig. 10 Photomicrographs of diagenetic processes. **a** B_{mic}—skeletal micritization, M—micritization and M_{env}—micritic envelope around the skeletal grain (sample KT/Ts-2). **b** M_{env}—micritic envelope around the crystalline grain (sample NW/Ts-5). **c** C_{iso}—isopachous fibrous cement, C_{mic}—micritic cement (sample KT/Ts-3). **d** C_{bk}—blocky calcite cement and C_{pio}—poikilotopic cement (sample KT/Ts-4). **e** C_{bk} —blocky calcite cement in vein filling (sample NW/Ts-6). **f** C_{gra}—granular mosaic cement (sample NW/Ts-2)

dissolution stage also constituted to the enlargement of the extensional fractures and cavern development where this process is the most prolific event of generating secondary porosity in the Sakesar Limestone (Fig. 11d, e). Thus, the dissolution in the Sakesar Limestone constituted three diagenetic environments, i.e., the marine, meteoric, and burial.

Neomorphism

The neomorphism in the Sakesar Limestone was noted on microscopic scale in almost all samples of the NGS and KTS. The aggrading neomorphism was noted in the Sakesar Limestone where recrystallization resulted in an increase in crystal sizes. The micritic matrix underwent from progressive and succeeding stages of diagenetic recrystallization

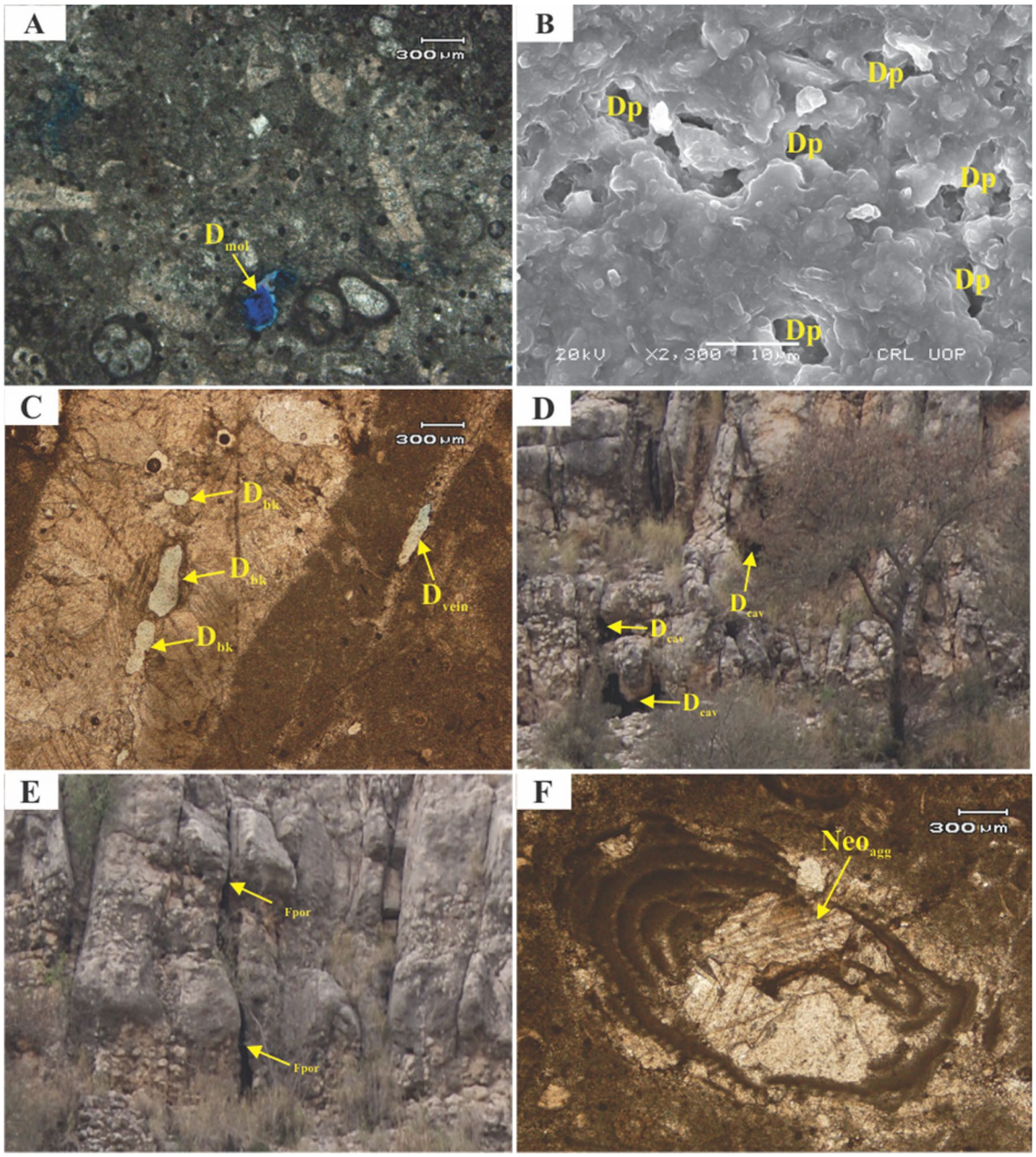

Fig. 11 Photomicrographs and outcrop photographs of diagenetic processes. **a** D_{mol}—dissolution of skeletal grain forming bimoldic porosity in sample NW/Ts-3. **b** The dissolution of micritic cement and formation of microporosity (Dp) in sample NW/Ts-4. **c** Selective dissolution of blocky calcite cement (D_{bk}) and selective dissolution of vein (D_{vein}) in sample KT/Ts-5. **d** Development of cavern porosity. **e** Enlargement of fracture porosity (F_{por}) by dissolution in later stage of uplift. **f** Aggrading neomorphism (Neo_{agg}) in the Sakesar Limestone (sample KT/Ts-4), the arrow from tail to head shows the full spectrum of aggrading neomorphism (micrite through blocky cement). Field photographs (**d**, **e**) are not to scale

into microspar and then into sparite (Fig. 11f; Khalifa et al. 2009). During the progressive stages of recrystallization in the Sakesar Limestone, the micrite is presented only by small irregular islands and ultimately led to the formation of blocky calcite cement (Fig. 11f; Abu-El Ghar et al. 2015). The aggrading neomorphism shows that the Sakesar Limestone has experienced marine to deep burial diagenesis. This type of neomorphism is well developed in the micritic matrix where coarser blocky calcite usually ensues in the centre and decreases towards the edges (Melim et al. 2002; Khalifa et al. 2009).

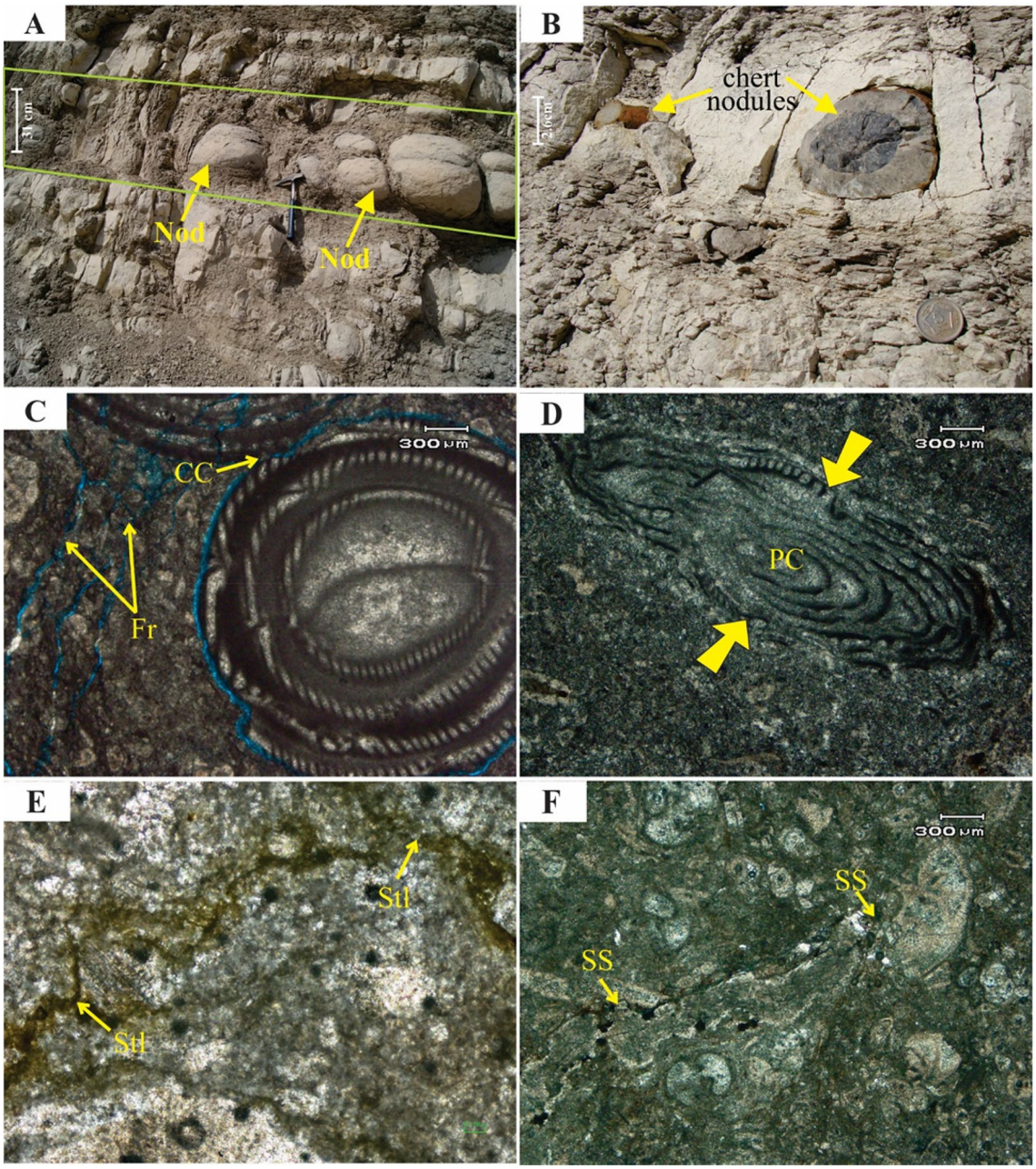

Fig. 12 Outcrop photographs of nodules and photomicrographs of diagenetic processes. **a** nodules (Nod) of limestone bounded by planar limestone beds at NGS. **b** Chert nodules in the Sakesar Limestone showing outer chert-poor and inner chert-rich zones. **c** Concave-convex contacts (CC) and fractures (Fr) in sample NW/Ts-4. **d** Physical compaction (PC), arrows indicate stress direction in sample NW/Ts-2. **e** Bedding-parallel stylolite (Stl) distinguished from surrounding due to iron oxidation in sample NW/Ts-6. **f** Solution seam (SS) formed by soluble phases precipitation in pore spaces of sample NW/Ts-3

Limestone nodularity

The nodular fabric in the Sakesar Limestone is observed on macroscopic scale in both the selected outcrop sections. These nodules of limestone are restricted to bedding at certain horizons and ranges from 5 to 30 cm and even large (Fig. 12a). According to Flügel (2010), the nodular fabric of limestone can be explained by diagenetic, sedimentary, and tectonic processes. Solution and cementation processes as well as nodule growth within the sediment are included in the diagenetic processes. Sedimentary nodules underline the role of transportation and redeposition. Tectonic processes explain the formation of nodular fabric by shear processes affecting limestone and marl/clay alternations. The origin of

nodular fabric in the Sakesar Limestone cannot be explained by a single mechanism as mentioned above. However, both diagenetic and tectonic processes support the origin of nodules in the Sakesar Limestone as predominant effects of pressure solution, alternating limestone and marl beds, and the deposition in tectonically active areas are prevailing conditions. Another more suitable explanation for the origin of nodular fabric in the Sakesar Limestone is believed to be the result of differential compaction or the concretional growth due to diagenetic differentiation of carbonate and argillaceous material (Ghazi et al. 2006).

Chert nodules- silicification

The chert occurs as nodular variety especially at the top of the Sakesar Limestone (Fig. 12b) and occasionally scattered in whole formation that varies in dimension from 5 to 10 cm and exceptionally up to 60 cm. These nodules are subequant to sub-circular which are oriented usually parallel to the nodular fabric in the Sakesar Limestone. The nodules have displayed two zones, i.e., the inner dark zone and outer light zone (Fig. 12b). These zones may involve geochemical variation in the concentration of precipitating silica and led to the formation of two distinct concentric structures of chert-rich and chert-poor zones. The inner zone represents the microcrystalline quartz chemistry probably flint while outer zone has still some calcite inclusions from the hosting Sakesar Limestone (Behl 2011). Despite of all, it requires further cathodoluminesence analysis that will provide high-resolution quantitative spectroscopy. The analysis of chert nodules will confirm the detrital and diagenetic modes of contributing minerals, provide clues for growth zonation and also establish silica cement stratigraphy for these chert nodules (Richter et al. 2003).

The possible genesis of nodular chert formation in the Sakesar Limestone is either through replacement of carbonate by silica or precipitation of pore-filling silica cement (Noble and Van Stempvoort 1989). One of the possible sources of silica for these nodules is believed to be the solution of siliceous biota in an early diagenetic stage at a shallow burial (Blatt et al. 1980). However, early mechanical compaction and sediment dewatering may have played a prime role in sponge dissolution, migration of silica rich fluid and the precipitation of silica in the Sakesar Limestone in the form of chert nodules (Ghazi et al. 2006).

Compaction

The compaction process affected the Sakesar Limestone after deposition that led to physical and chemical rearrangements and variations in the bulk volume of sediments. All the physio-chemical changes through compaction in the Sakesar Limestone are divided into two types, i.e., mechanical compaction and chemical compaction (Table 2; Figs. 2, 3 and 12c–e).

Mechanical compaction In the Sakesar Limestone, mechanical compaction is much more evident in wackestone–packstone microfacies. The mechanical compaction is noted in the samples NW/Ts-1, NW/Ts-2, NW/Ts-4 and NW/Ts-7 in the NGS and KT/Ts-3, and KT/Ts-5 in the KTS. The order of the observed features of mechanical compaction includes closer packing of grains, close grain contacts and decrease of primary interparticle porosity in grain-supported limestones (Figs. 12c, d; Mahboubi et al. 2010). The grains and even matrix have been squeezed because of tectonic load that results in closer packing of sediments (Fig. 12d). When the brittle or ductile strength of the grains and matrix exceed, then breaking of grains and fracturing take place (Fig. 12c). Mechanical compaction also declines porosity and substantial reduction of sediment thickness occurs through closer packing and sediments squeezing (Vincent et al. 2007). Meanwhile, the development of late stage fracturing subsequently enhanced almost all porosities. It is difficult to say whether this period of fracturing may be the result of shallow burial or uplift in deep burial realm of sediments but overall fracturing event postdates stylolites and, in this case, represents deep burial realm.

Chemical compaction: pressure solution (stylolites) The spectrum of chemical compaction features in the Sakesar Limestone are Stylolites and solution seams which are noted in samples NW/Ts-1, NW/Ts-3, NW/Ts-4 and NW/Ts-6 in the NGS. The stylolitization is one of the wide spread diagenetic events present in carbonate reservoirs of the world (Oswald et al. 1995; Morad et al. 2012; Alsharhan and Sadd 2000) which is the result of limestone texture, mineralogy and facies and affects reservoir characteristics (Andrews and Railsback 1997; Baron and Parnell 2007; Vandeginste and John 2013). The stylolitization is a very important diagenetic event in the Sakesar Limestone and frequently took place where the bedding parallel stylolites types are recognized (Fig. 12e; Paganoni et al. 2016). The bedding parallel stylolites are of high amplitude undulations which are parallel to sub-parallel to the bedding and may form by dissolution along bedding surfaces (Park and Schot 1968; Logan 1984; Tondi et al. 2006; Paganoni et al. 2016) which was triggered by increase in overburden pressure (Rolland et al. 2014; Ben-Itzhak et al. 2014) and are typical stylolites of the Sakesar Limestone (Fig. 12e). The bedding parallel stylolites are very conspicuous because of the infilling or coating of iron oxides enrichment and help to distinguish stylolites from the surroundings (Fig. 12e). The pressure solution seam is another diagenetic feature in the Sakesar Limestone that develops as a result of dissolution at stressed

grain contacts followed by dispersal and elimination of the dissolved material from interstitial fluids and ultimately the precipitation of soluble phases at cracks and pores that preserve in the form of stylolitic seams (Fig. 12f; Nenna and Aydin 2011; Viti et al. 2014). The stylolitization manifests that the Sakesar Limestone has experienced shallow burial diagenesis.

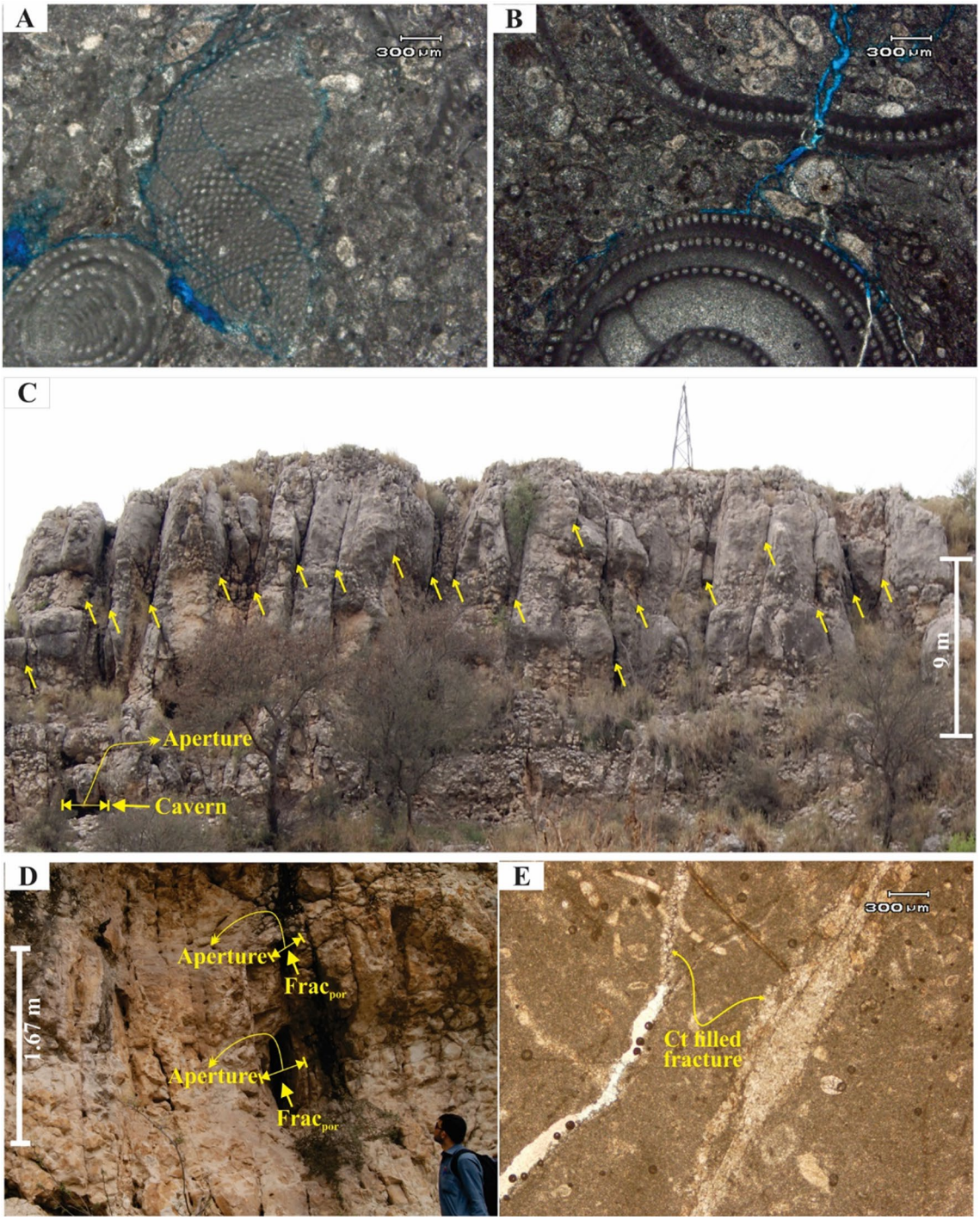

Fig. 13 Photomicrographs and outcrop photographs of diagenetic processes. **a** Intragranular microfractures that confined to singular grain in sample NW/Ts-4. **b** Transgranular microfractures in Alveolina-algal packstone microfacies (sample NW/Ts-4). **c** Extensional fractures that are associated with folding phenomena in the Sakesar Limestone at KTS. Arrows showing the position of extensional fractures, in the lower left portion a small cavern is shown. **d** Extensional fracture aperture size at KTS. **e** Calcite filled fractures and selective dissolution of vein in wackestone microfacies (sample KT/Ts 5)

Fractures and veins

The fracturing and vein observed on microscopic and macroscopic scale in the studied sections of the Sakesar Limestone are shown in Figs. 13a–e. The observed microfractures are divided into two types on the basis of their fracturing intensity limit to singular or multiple grains; (a) the intragranular microfractures if they only affect a single grain (Fig. 13a), (b) intergranular or transgranular fractures that transect several grains (Fig. 13b; Passchier and Trouw 2005). The macrofractures observed in the Sakesar Limestone are mostly extensional fractures (Fig. 13c). These fractures may be tectonic fractures associated with folding, regional fractures are normal to the bedding planes and contraction fractures are either tensional or extensional fractures associated with bulk volume reduction (Ahr 2008).

In the fractured carbonate reservoirs, the movement of fluids primarily depends upon the pore types, internal fracture network and the connectivity of pores (Loucks et al. 2012). Carbonate fractured reservoirs are usually homogeneous where development of a network of fluid-transmitting fractures is controlled by the local stresses, mechanical properties, and layering of the various lithotypes, as well as their spatial distribution (Larsen et al. 2010). In the Sakesar Limestone, fractures and veins are abundant which are evident on outcrop as well as on microscope scale. The vertical fractures at outcrop scale are characteristic features at KTS (Fig. 13c). The aperture of fractures varies in size and becomes enlarge where fractures are associated with dissolution (Figs. 13c, d). The microfractures were converted to veins during deep burial diagenesis by the infilling of calcite cement where mostly the blocky calcite cement precipitated (Fig. 13e). These veins may also have dissolved selectively in deep burial diagenesis (Fig. 11c).

Reservoir characterization

The qualitative and quantitative reservoir analysis of the Eocene Sakesar Limestone from outcrop data is achieved by implementing petrographic studies. The petrographic analysis on microscopic and mesoscopic scale analysis is considered to recognize the porosity types and then porosity classification model for the Sakesar Limestone is proposed. The core plug analysis is utilized for the accurate quantitative measurements of porosity and permeability from outcrop data of the Sakesar Limestone.

Table 3 Recognized porosity types in the Sakesar Limestone

Sample #	Intraparticle/ intracrystalline	Interparticle/ intercrystalline	Moldic/ solution	Fracture
NW/Ts-7	–	–	–	✓
NW/Ts-6	✓	✓	–	–
NW/Ts-5	–	–	–	✓
NW/Ts-4	–	✓	✓	✓
NW/Ts-3	–	–	✓	✓
NW/Ts-2	–	✓	✓	–
NW/Ts-1	–	–	–	✓
KT/Ts-5	–	–	–	✓
KT/Ts-4	–	–	–	✓
KT/Ts-3	–	–	✓	✓
KT/Ts-2	–	–	–	–
KT/Ts-1	–	–	–	✓

The presence of respective porosity types are shown by tick marks

Porosity

Three approaches are utilized to characterize the pore types in the Sakesar Limestone, i.e., microscopic, mesoscopic and plug porosity and permeability.

Microscopic porosity The recognized microscopic porosity types are shown in Table 3. These microscopic porosities are grouped together according to the recognized microfacies. The intraparticle porosity is identified from both NGS and KTS in the perforate larger benthonic foraminifera which is mostly filled by micritization or neomorphic cement (Fig. 14a). The interparticle porosity is noted in samples NW/Ts-6 and NW/Ts-4 of SLF-1 and SLF-5 microfacies, respectively (Fig. 14b). The moldic porosity is identified in samples NW/Ts-4 of SLF-5 microfacies, NW/Ts-3 and NW/Ts-2 of SLF-2 microfacies. The solution porosity is noted and divided as matrix solution porosity where fluid chemistry undersaturated with respect to $CaCO_3$, dissolving the cementing material and forming intercrystalline solution pores and biomoldic porosity (Fig. 14c, d). The most dominant microporosity type is fracture and or stylolitic porosity which is formed in almost all microfacies of the Sakesar Limestone and is divided into anastomosing network fracture/stylolitic porosity and bedding-parallel fracture porosity (Fig. 14e, f). The visually estimated average microporosity of the Sakesar Limestone for the NGS varies between 0.54 and 2.05% and 0.35–0.88% for the KTS.

The dominantly identified microporosity types in the Sakesar Limestone contribute to the secondary origin except scarcely noted intraparticle porosity that owe to be primary depositional porosity. The fracture porosity is the most commonly identified secondary porosity type in the Sakesar Limestone that plays a dynamic role in the development

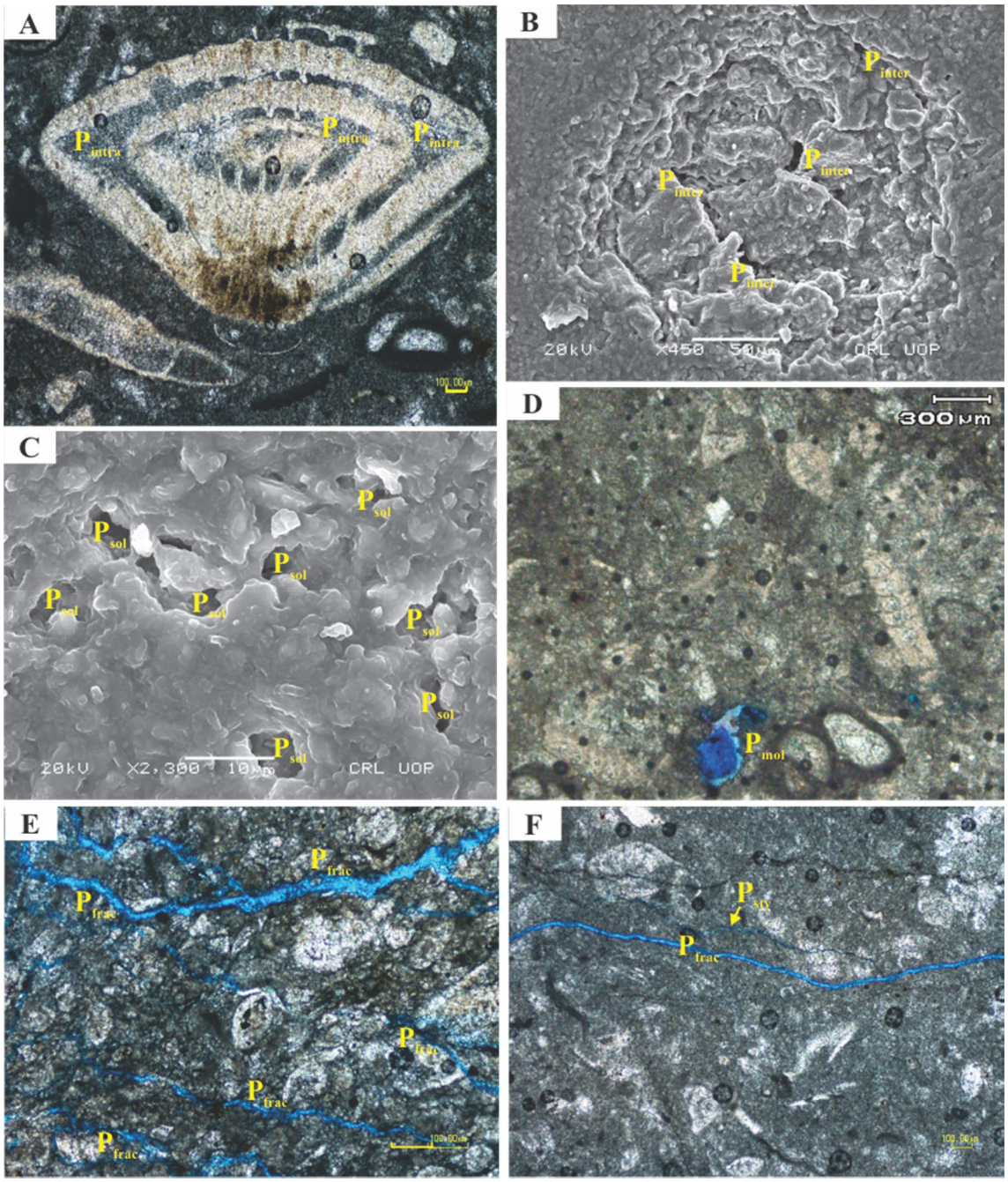

Fig. 14 Photomicrographs showing different types of microporosity. **a** Calcite filled intraparticle porosity (P_{intra}) in *Nummulites* of sample NW/Ts-5. **b** SEM photomicrograph showing intercrystalline porosity (P_{inter}) in benthonic foraminiferal wackestone microfacies of sample NW/Ts-6. **c** Solution porosity (Psol) in wackestone microfacies (sample NW/Ts-4). **d** Moldic porosity (P_{mol}) in algal-miliolidal wackestone microfacies (sample NW/Ts-3). **e** Fracture porosity (P_{frac}) in alveolina rich packstone microfacies (sample NW/Ts-4). **f** Bedding-parallel fracture porosity (P_{fra}) and re-opened stylolitic porosity (P_{sty}) in wackestone microfacies (sample NW/Ts-7)

of porosity and establishing fluid flow paths in the Sakesar Limestone.

Carbonate microporosity classification The various types of carbonate porosities are the ultimate results of three types of processes, i.e., depositional, diagenetic and fracturing. These three processes are considered to plot as end members on a triangular diagram with notations about hybrid pore types on its sides. The end member processes are independent but hybrid pore types exist between them because more than one mechanism can affect the formation of a given pore system at different times during its genetic history. This new genetic carbonate porosity classification scheme is proposed

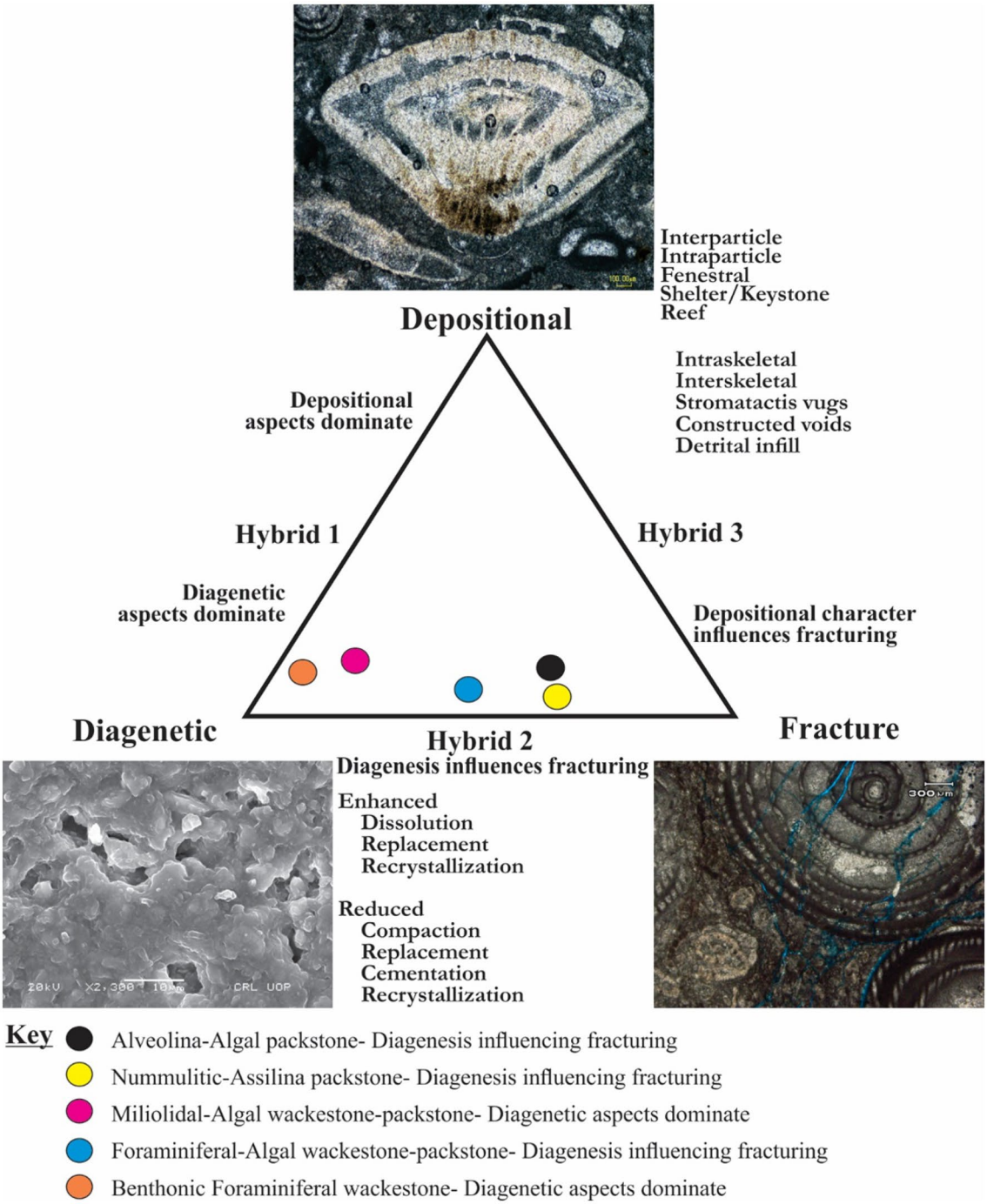

Fig. 15 A genetic classification model of porosity for the Sakesar Limestone at NGS and KTS (modified after Ahr 2008)

by Ahr (2008). According to this classification, the dominant characteristics of any of these processes are used as reliable proxy for porosity generation and in this way spatial distribution of porosity may not be restricted to depositional facies boundaries. This classification is used in the present research work to delineate different carbonate porosity types in the Sakesar Limestone.

According to Ahr (2008) classification, the identified carbonate porosity types of the Sakesar Limestone have been shown in Fig. 15. The benthonic foraminiferal wackestone and Miliolidal-Algal wackestone–packstone

constitute pores where diagenetic aspects dominate. Foraminiferal-Algal wackestone–packstone consists of pores which are hybrid of diagenetic and fracture processes whereas Nummulitic-Assilina packstone and Alveolina-Algal packstone constitute pore types which are predominantly consist of fracture porosity (Fig. 15).

Mesoscopic porosity The obvious mesoscopic or outcrop scale porosity of the Sakesar Limestone is identified by the presence of fractures and small caverns. These mesoscopic scale porosities are evident at KTS and identified by unique type of vertical extensional fractures that are thoroughgoing from top to bottom (Fig. 13c, d). These fractures are mostly open fractures that may play an ideal role to establish fluids flow paths for the hydrocarbons and may assist to make the Sakesar Limestone as permeable horizons. The detail fracture analysis is not carried out; however, size of the aperture/openings is calculated for these fractures. The size of aperture in these vertical fractures ranges from 2 to 30 cm and in places it may exceed than this as shown in Fig. 13c. These vertical fractures are typically associated with the folding of the Sakesar Limestone prior to faulting (Jadoon et al. 2005). Some small cavern porosity is also noted in the Sakesar Limestone (Fig. 13c) and this is one of the major clues for the carbonate reservoir higher storage capability that evolved because of dissolution process. The aperture size in the cavern ranges from 1–3.5 ft (Fig. 13c, d). Thus, the presence of extensional fractures and small cavern may add to the mesoscopic porosity of the Sakesar Limestone. The extension fractures enhance both total porosity and permeability. The small caverns only add to the porosity of the Sakesar Limestone.

Plug porosity and permeability The quantitative porosity and permeability precisely measured from outcrop plug analysis because normally, estimated visual porosity from petrographic analysis provides exaggerated porosity values. The plug porosity and permeability of selected samples (i.e., NW/TS-2, NW/TS-4 and CSS/TS-1) of both outcrop sections were carried out. The estimated porosity from these samples ranges from 0.879 to 2.899% (Table 4) while measured permeability values for these selected samples range from 0.013 to 0.028 mD (Table 4). The tomography of plug porosity and permeability of the selected samples is shown in Fig. 16a, b. The plug porosity shows a positive correlation coefficient ($r = 0.4947$) with plug permeability. The linear regression equation of $y = 0.0037x + 0.0138$ has been calculated for the plug porosity and permeability values in order to fit a regression line to the set of points of plug porosity and permeability (Fig. 16c).

Table 4 The plug porosity and permeability data of the selected outcrop samples

S. no	Sample	Microfacies	Porosity (%)	Permeability (mD)
1	NW/TS-2	SLF-5	1.811	0.028
2	NW/TS-4	SLF-2	2.899	0.021
3	CSS/TS-1	SLF-1	0.879	0.013

Discussion

Depositional model

The constituting abundant skeletal allochems, the abundant micrite matrix, the vertical distribution of microfacies, associations of various fauna and flora and interpreted depositional environments of individual microfacies of the Sakesar Limestone enhance overall deposition in shallow marine, subtidal, semi-restricted lagoonal conditions of inner to middle ramp settings (Fig. 17). In the present case, the distribution of various larger benthonic foraminifera and dasycladale algae in combination with other bioclasts has been meditated to deduce the depositional environment of these dominantly micritic limestones.

During Eocene time, there was abundance of miliolids and larger benthic foraminifera, predominantly *Nummulites, Assilina, Alveolina* and *Discocyclina* sp. (Mehr and Adabi 2014). *Nummulites* employed broader range of open marine environments on inner to middle and even outer ramp settings, and was usually absent from more restricted waters (Racey 2001; Beavington-Penney and Racey 2004). Smaller lenticular to sub-globular *Nummulites* ensue in shallow waters of inner ramp settings often along with *Alveolina* sp., miliolids and Dasycladale algae, whereas large flat and discoidal *Nummulites* with equally shaped *Assilina* sp. occur in comparatively deeper water of middle to outer ramp settings (Racey 2001; Beavington-Penney and Racey 2004; Vaziri-Moghaddam et al. 2006; Barattolo et al. 2007; Payros et al. 2010; Mehr and Adabi 2014). *Nummulites* with medium to large sized, lenticular to globular form tend to inhabit intermediate ramp settings (Adabi et al. 2008). These regional patterns with minor modifications are also involved in several ancient ramps (e.g., Racey 1994; Sinclair et al. 1998). The idealized faunal associations along carbonate ramp settings during Eocene time were suggested by Racey (1994). Based on this model, Textulariids, miliolids and Dasycladale algae occur in the shallowest part of the inner ramp, while Nummulites and Assilina with minor Alveolina and Dasycladale algae occur in the deeper parts of middle ramp settings. This faunal association is characteristic of shallow-marine, benthic communities prevailed in tropical to sub-tropical

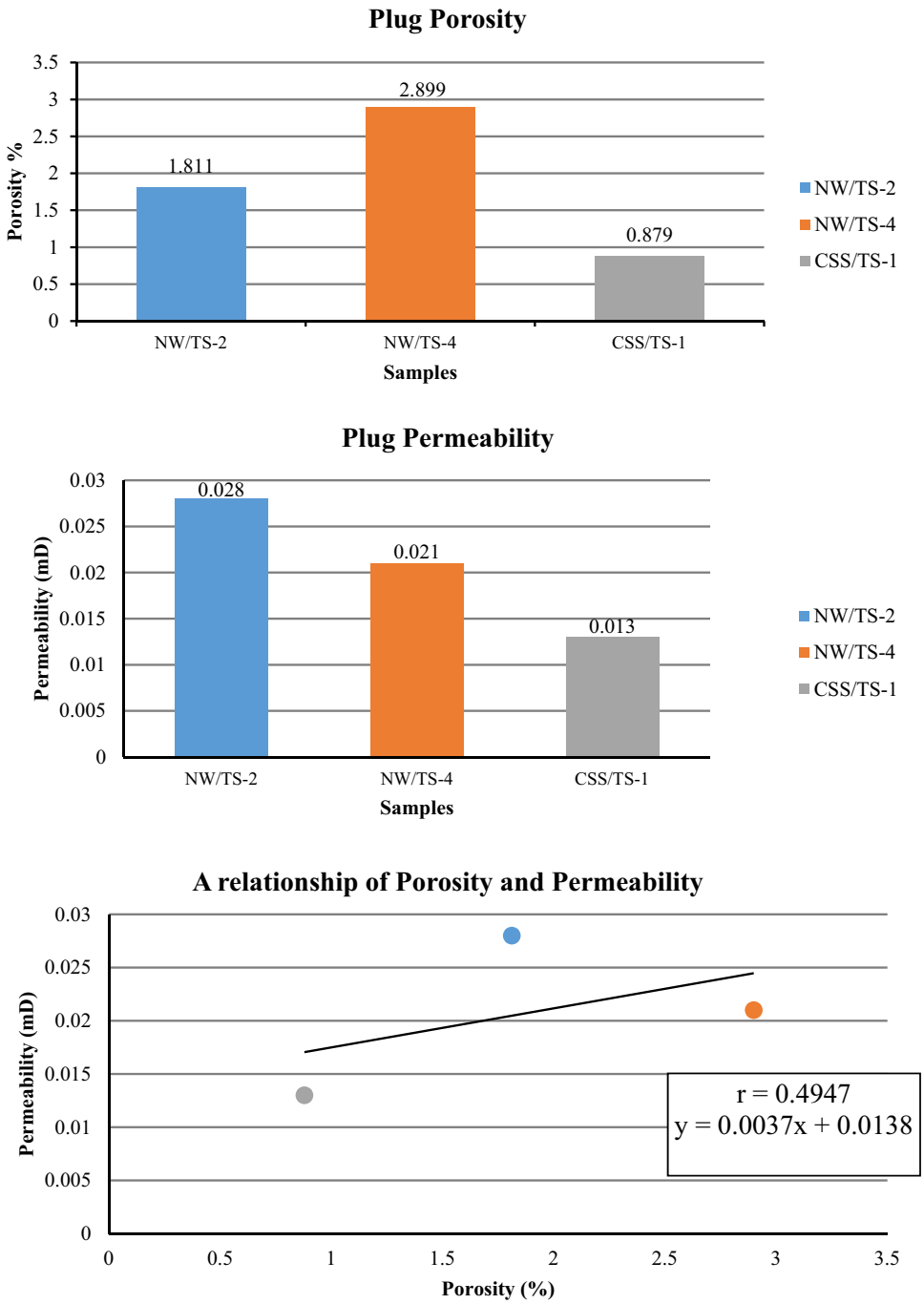

Fig. 16 Porosity–permeability graphs. **a**, **b** Tomography of the plug porosity and permeability for the selected samples. **c** The plug porosity and permeability relationship in the selected samples

modern marine carbonate environments. In the proximal part of inner ramp setting the ratio of imperforate to perforate benthonic foraminifera is high while towards the distal part of the middle ramp this ratio decreases (Racey 2001). Thus, the larger foraminifera are valuable tools to model paleoenvironments and reservoir potentiality in shallow-marine settings (Geel 2000; Racey 2001) and used as outstanding indicators for the interpretation of facies (Rasser et al. 2005; Mehr and Adabi 2014). The benthonic foraminifera and algae were key producers of carbonates in shallow-marine ramp setting during Eocene time throughout the world (Racey 2001; Wilson and Vecsei 2005; Payros et al. 2010; Mehr and Adabi 2014). The abundance of benthonic foraminifera in all identified microfacies specifies deposition within the photic zone. Today, benthonic larger foraminifera are confined to photic zone, since all of them have symbiotic relationship with algae. The dispersal of these foraminifera within photic gradient is restricted by temperature and nutrient supply regarding greater depth, photo-inhibition and high salinity at the sea

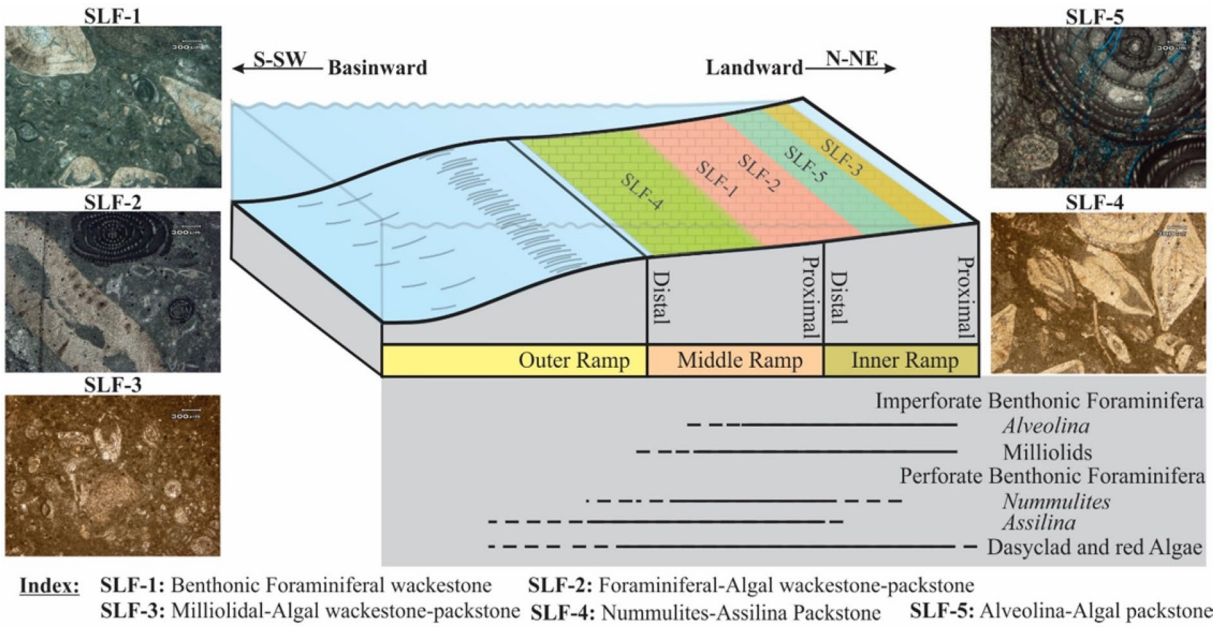

Fig. 17 The schematic distribution of selected imperforate and perforate benthonic foraminifera along carbonate ramp (after Racey 1994; Gilham and Bristow 1998; Beavington-Penney and Racey 2004) and a proposed depositional model of the Sakesar Limestone for the NGS and KTS (modified after Flügel 2010)

surface (Hottinger 1997; Hohenegger 2000, 2004; Barattolo et al. 2007). The nummulites indicates eutophic to oligotrophic conditions as most of their energy is thought to derive from their symbiotic algae (Beavington-Penney and Racey 2004; Swei and Tucker 2012). However, the dasycladale algae occurs in warm water of shallower depths not more than a few meters where low water agitation predominantly in semi-restricted lagoonal and ramp settings favors the presence of green algae (Heckel 1972; Wray 1977; Dodd and Stanton 1981; Reeckmann and Friedman 1982; Granier 2012).

The existence of larger benthonic foraminifera in the Sakesar Limestone of Salt Range shows the perseverance of tropical to sub-tropical climate during deposition of this formation as compared to other Tethyan carbonate ramps (Buxton and Pedley 1989). Based on various established microfacies associations identified in the Sakesar Limestone, the gentle-dipping foraminiferal-Algal dominated carbonate ramp depositional model is suggested for this formation (Fig. 17). The ramp setting for Sakesar Limestone is propped by the absence of reef builder organism, the higher occurrences of micrite in all microfacies, lack of resedimentation, absence of high-energy grainstone microfacies, and gradual inclination of shallow platform towards basin, are more compatible with a ramp setting than a shelf (Wright 1986; Mehr and Adabi 2014).

The Sakesar Limestone is divided into inner ramp and middle ramp according to Racey (1994) and Gilham and Bristow (1998). The inner ramp settings are categorized by miliolids and *Alveolina* sp. dominated microfacies types while in middle ramp, the dominant microfacies are of *Nummulites* and *Assilina* sp. In the present study, there was absence of high-energy oceanic currents (Puga-Bernabéu et al. 2010; Payros et al. 2010) where the biotic association of microfacies and paleolatitude undoubtedly recommends a tropical–subtropical depositional setting for the Sakesar Limestone. The interpreted environments and their vertical variations are shown in Figs. 2 and 3. These variations demonstrate that asymmetric cyclic deposition took place and shows that most of the limestone was formed during depositional regression.

Paragenetic sequence and diagenetic environments

The sequence of diagenetic processes in carbonates relies on sediment, grains size and their texture, mineralogy, nature of pore fluid and climate conditions (Tucker and Wright 1990; Flügel 2010). Based on the diagenetic features, mineralogical compositions, cement types and occurrences, as well as main microfabrics, diagenetic environments of the Sakesar Limestone were distinguished and assigned as marine, meteoric, burial and uplift realms. Each of these diagenetic environments has specific characteristics and diagnostic features which are briefly discussed in the following lines. The paragenetic sequence and the diagenetic model for the Sakesar Limestone are shown in Figs. 18 and 19, respectively.

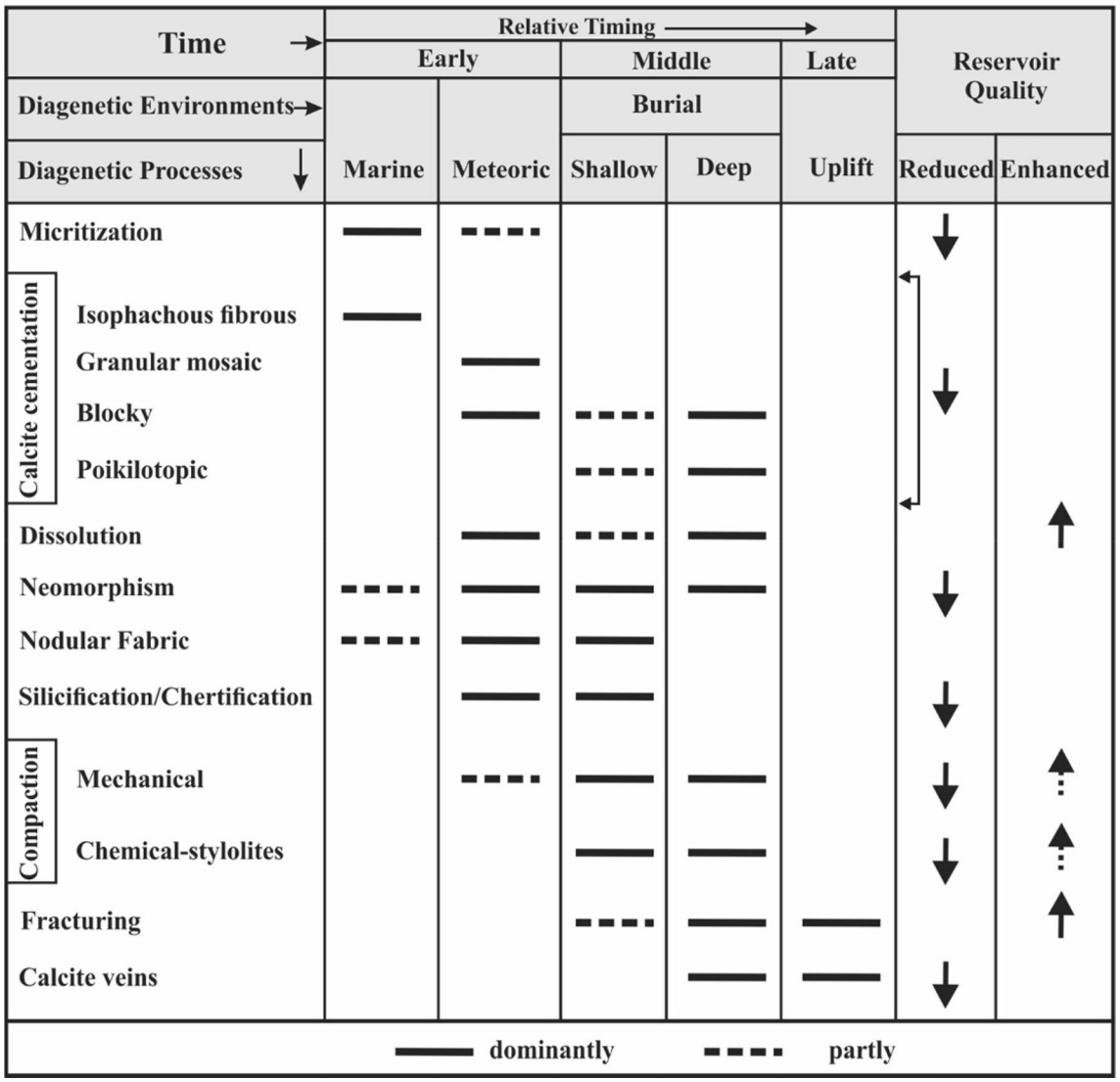

Fig. 18 The paragenetic sequence and the reservoir quality decreasing and increasing diagenetic events of the Sakesar Limestone in the study area

Marine Environment

Marine diagenetic environments are recognized by first generation of micritization, non-ferroan isopachous fibrous cements (Melim et al. 2001; Khalifa 2005; Taghavi et al. 2006; Vincent et al. 2007; Esrafili-Dizaji and Rahimpour-Bonab 2009; Mahboubi et al. 2010; Tavakoli et al. 2011; Abu-El Ghar et al. 2015). The micritization is the prominent diagenetic feature identified in the Sakesar Limestone and is likely to be formed in marine environment. The micritization in the Sakesar Limestone is very severe and is observed in the form of micritic envelopes and skeletal micritization (Fig. 10a, b) that may have been formed because of mechanical disintegration or bioerosion of the large calcareous biota, e.g., Nummulites/algae by endolithic algae (Melim et al. 2002; Abu-El Ghar and Hussein 2005; Khalifa 2005).

Meteoric environment

The granular mosaic cement, early stage of blocky cement, dissolution of molds and micritic cement as well as polymorphic transformations (neomorphism) of primary marine minerals all are signs of the meteoric-phreatic diagenetic realm (Melim et al. 2001; Khalifa 2005; Vincent et al. 2007; Moradpour et al. 2008; Khalifa et al. 2009; Esrafili-Dizaji and Rahimpour-Bonab 2009; Mahboubi et al. 2010; Tavakoli et al. 2011; Abu-El Ghar et al. 2015). During the meteoric-phreatic stages, metastable skeletal and non-skeletal grains are dissolved, creating secondary fabric- and

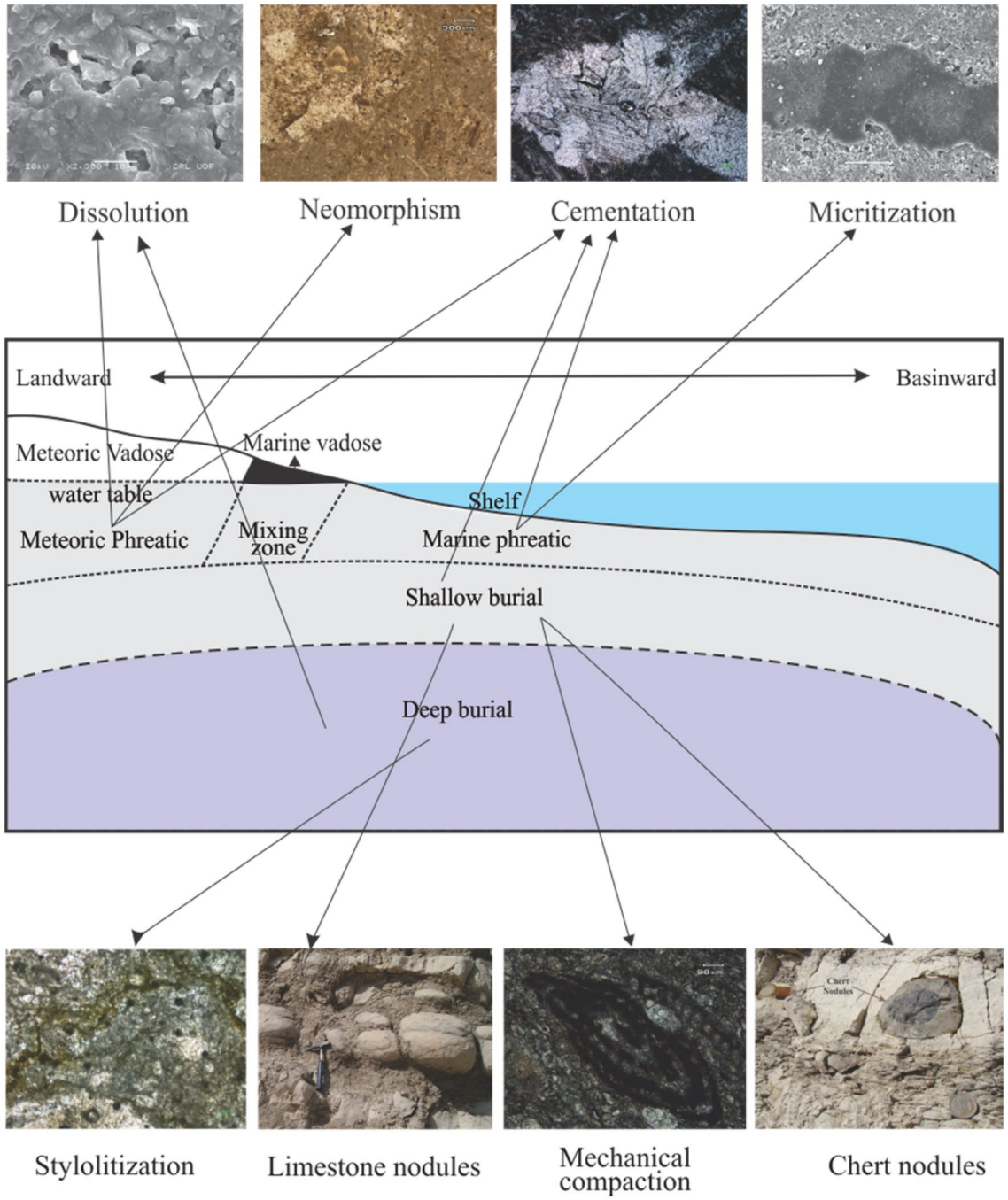

Fig. 19 The simplified scheme of major diagenetic environments proposed for the Sakesar Limestone, a typical carbonate ramp (modified after Flügel 2010)

non-fabric selective porosity such as intercrystalline, intraparticle and moldic/solution porosities (Abu-El Ghar et al. 2015; Fig. 14c–f). The neomorphism is very common and severe in the Sakesar Limestone that has been observed in almost all microfacies. The observed neomorphism is of aggrading type because it ultimately led to the formation of blocky calcite cement that shows different crystal sizes from microspar into blocky calcite cement. The ferroan cement is rarely formed along stylolitic sutured surfaces that represent precipitation in reducing meteoric or burial environment (Fig. 12e).

Burial environment

The observed diagenetic features show that the Sakesar Limestone have been passed through burial diagenesis.

Mechanical compaction, silicification, recrystallization, limestone nodularity and chemical compaction indicate an overall burial diagenetic realm (Mahboubi et al. 2010) for the Sakesar Limestone and their petrographic characteristics include sutured and concave-convex contacts, fractures and veins, chert nodules, blocky and granular calcite cements, stylolites and solution seams and nodular fabric of limestone. The burial diagenetic realms are conventionally segmented into shallow burial and deep burial; however, the exact boundary is not well defined (Vincent et al. 2007; Flügel 2010). The mechanical compaction features such as sutured and concave–convex contacts represent shallow burial realm (Vincent et al. 2007; Mahboubi et al. 2010). The mechanical compaction is also susceptible to variable porosity reduction (Abuseda et al. 2015). The chert nodules formed as replacement of carbonate by siliceous precipitation of pore-filling silica or as siliceous biota solution precipitation in the initial diagenetic stage at a shallow burial (Blatt et al. 1980; Noble and Van Stempvoort 1989). The chemical compaction features such as stylolites and solution seams are the characteristic features of shallow burial realm (Vincent et al. 2007; Mahboubi et al. 2010; Abuseda et al. 2015). The diagenetic and tectonic processes together support the origin of nodular fabric. The development of fractures, veins, blocky calcite with undulatory extinction, poikilotopic cement and later stage of selective dissolution of blocky cement and vein formed in deep burial realm.

Uplifting

Late diagenetic events affected the Sakesar Limestone after uplifting that resulted in the formation of fractures by the Alpine-Himalayan orogenies when the basin was folded and faulted during Eocene time. Some fractures have been occupied with calcitic cement. Dissolution and fracturing are the most important processes that helped to create secondary porosity in this interval.

Impact of diagenesis on reservoir quality

From petrophysical aspect, the diagenesis is the key controlling factor on the reservoir quality that plays dual constructive and destructive role upon the pore volume storage capability and hence on the potentiality of reservoir rock (Taghavi et al. 2006; Tavakoli et al. 2011; Abuseda et al. 2015). The dual diagenetic behavior makes the carbonate reservoir heterogeneous that pronounces how much and how rapidly properties vary from place to place (Kennedy 2015). The heterogeneities in the petrophysical properties caused by the diagenetic processes have profound impact on the reservoir quality of the Sakesar Limestone. These diagenetic processes are categorized into two groups in order to show the impact of diagenesis on reservoir quality of the Sakesar Limestone (as shown in Fig. 18). These processes are as follows:

Reservoir quality reducing diagenetic processes

- The micritization is the most dominant diagenetic process in the Sakesar Limestone that preserved in the forms of endolithic micritic envelopes around the grains as well as partial or complete skeletal micritization (Fig. 10a, b). This process led to the infilling of intraparticle and interparticle porosity and reducing permeability by decreasing pore throat size (Taghavi et al. 2006). Hence, micritization negatively impacts the potentiality of the Sakesar Limestone.
- The cementation in the Sakesar Limestone is the main diagenetic mechanism that reduced porosity and permeability (Fig. 10c–f). The major porosity obstructing cements precipitated in the early diagenetic history of the Sakesar Limestone where intraparticle and interparticle pore spaces filled by the calcite cements and diminishing the reservoir potentiality (Esrafili-Dizaji and Rahimpour-Bonab 2009). The impact of cementation on reservoir permeability is very obvious. The facies that has more than 10% calcite cement are low permeable comparative to other facies (Cantrell and Hagerty 2003). The later diagenetic blocky calcite cement filled the fractures where cement minimized the flow pathways of the fluids by reducing pore throats and in this way reduces reservoir quality of the Sakesar Limestone (Fig. 10e; Westphal et al. 2004).
- The noted aggrading neomorphism in the Sakesar Limestone results in the transformation of original aragonitic/calcitic micrite into microsparite to sparite (Fig. 11f). Theoretically, the transformation of aragonite to calcite results in increase of 8% in rock bulk volume that ultimately decreases 8% porosity (Selley 2000). The aggrading neomorphism is the key porosity-reducing factor in the Sakesar Limestone that caused lessening of the intercrystalline pore spaces through growth of larger crystals that interfere and destroy the interstitial pore spaces (Abuseda et al. 2015).
- The mechanical compaction contracts the bulk volume of the rock due to overburden or lithostatic pressure as sediments undergoes burial that result in the formation of closer packing, squeezed grains, sutured contacts and hence, tight/packed rock pattern formation. As these features form, the intergranular and intragranular porosities as well as permeability are either completely diminished or pore throats decrease in size. Hence, all these features show that mechanical compaction reduces the reservoir quality of the Sakesar Limestone.
- The silicification or chertification event of the Sakesar Limestone is one of the diagenetic events that possibly

destroys the reservoir quality. The chert nodules form mechanical stratigraphic unit intervals that give stability to the Sakesar Limestone. These unit intervals then lead to the reduction of fracture density as well as deflection of fractures at chert nodule horizons where these nodules reduce connectivity of fractures and, in this way, minimize the fluid flow paths (Spence and Finch 2014). The impact of chert nodules is more pronounced in the incompetent horizons of the Sakesar Limestone as compared to the tighter horizons.

- The chemical compaction or stylolitization (compactional) that completely or partially destroys porosity and eliminates permeability as a result of pressure dissolution (Fig. 12e) where pores are either developed as primary or during earlier diagenetic history (Ferket et al. 2003). They may also act as seals where there is the presence of solution seams that obstructing fluid circulation (Fig. 12f; Ehrenberg et al. 2006; Moradpour et al. 2008). Hence, stylolitization process destroys the reservoir quality of the Sakesar Limestone.

Reservoir quality enhancement diagenetic processes

- The dissolution is one of the major diagenetic events in the Sakesar Limestone that resulted in the expansion of intergranular pores and the development of molds (Figs. 11b–d, 14c, d; Abuseda et al. 2015). The dissolution process enhances the porosity of the Sakesar Limestone as it has played a major role in the formation of various types of porosities which are moldic, matrix solution and cavern porosity that lead to the enlargement of pores. Therefore, the dissolution event in the Sakesar Limestone positively impacts on reservoir quality.
- The microscopic and mesoscopic dominant event in the Sakesar Limestone is fractures as noted from almost all samples and in outcrop sections that facilitate fracture porosity (Figs. 13a–d, 14e). These fractures not only enhance the storage capacity of the Sakesar Limestone but it also enhances permeability for the movement of hydrocarbon fluids (Ferket et al. 2003). So, the impact of fracture event in the Sakesar Limestone is positive on reservoir quality.
- Due to the tectonic impact, some of the stylolites reopening took place with the development of fluid flow channels (permeability) and stylolitic porosity (Fig. 14f). Hence, the tectonic stylolites may also have some input to enhance reservoir potentiality in the later part of the burial uplift by increasing permeability and total porosity of the Sakesar Limestone (Ferket et al. 2003; Hassan 2007).

Thus, the present diagenetic evolution of the Sakesar Limestone has shown that porosity of the Sakesar Limestone is mostly secondary in origin and developed during dissolution and fracturing phases of diagenesis. The marine diagenetic events of micritization and cementation reduced reservoir characteristics. Most of the reservoir characteristics improved in the meteoric realm, i.e., during shallow burial and prior to the onset of pressure-solution where dissolution and fracturing are the dominant reservoir enhancing diagenetic processes. The stylolites formation in the burial environment mostly reduces the reservoir quality of the Sakesar Limestone; however, later reopening of the stylolites adds to improve reservoir quality. In the deep burial environment, the predominant reservoir enhancing process is fracturing associated with folding that generates extensional fractures. The dissolution of calcite cement and widening of fractures in the deep burial environment further add to the reservoir potentiality of the Sakesar Limestone.

Conclusions

- In the Sakesar Limestone, five microfacies were recognized (i.e., Benthonic Foraminiferal wackestone, Foraminiferal-Algal wackestone–packstone, Miliolidal-Algal wackestone–packstone, Nummulitic-Assilina packstone and Alveolina-Algal packstone) which are interpreted to be deposited in the proximal inner ramp to distal middle ramp environment.
- The diagenetic fabric has been elucidated and on that basis paragenetic sequence has been established (i.e., micritization, cementation, dissolution, neomorphism, limestone nodularity, silicification, mechanical compaction, chemical compaction, and fractures and veins). These diagenetic events have manifested that the Sakesar Limestone have practiced marine, meteoric, burial and uplift realm diagenesis.
- The genetic porosity types (i.e., depositional, diagenetic and fracture) have been recognized but fracture porosity evolved as dominating porosity type. The other porosity types recognized include moldic (solution), intraparticle, intercrystalline.
- The core plug porosity and permeability relationship is verified by medium positive correlation coefficient and linear regression that support higher values of porosity for higher values of permeability.
- The impact of diagenesis and sedimentology displayed that the Sakesar Limestone is a reservoir of secondary origin. The diagenesis aided its vital role to make it prolific hydrocarbon pool.

- The fractures and dissolution enhance the reservoir potential of the Sakesar Limestone and make it a prolific hydrocarbon pool while all the other diagenetic events destroy its reservoir quality.
- The fractures have established the flow paths for the migration and accumulation of fluids and demonstrate that permeability is more important in the Sakesar Limestone than the total porosity.

Acknowledgements The authors are thankful to the National Centre of Excellence in Geology (NCEG), University of Peshawar for sponsoring this research work. The authors are also grateful to CRL, University of Peshawar for conducting SEM studies. HDIP is also acknowledged by the authors for plug porosity and permeability analysis.

References

Aamir M, Siddiqui MM (2006) Interpretation and visualization of thrust sheets in a triangle zone in eastern Potwar, Pakistan. Lead Edge 25:24–37

Abu-El Ghar M, Hussein A Post-depositional changes of the lower-middle eocene limestones of the area between Assiut and Minia, West of the Nile Valley, Egypt. In: Proceedings of the first international conference on the geology of the Tethys, 2005. Cairo University Press, pp 224–248

Abu-El Ghar MS, Khalifa M, Hussein A (2015) Carbonate diagenesis of the mixed clastic–carbonate Galala Formation, North Eastern Desert, Egypt. Arab J Geosci 8:2551–2565

Abuseda H, Kassab MA, LaLa AM, El Sayed NA (2015) Integrated petrographical and petrophysical studies of some Eocene carbonate rocks, Southwest Sinai, Egypt. Egypt J Petrol 24:213–230

Acharyya S (2007) Evolution of the Himalayan Paleogene foreland basin, influence of its litho-packet on the formation of thrust-related domes and windows in the Eastern Himalayas–A review. J Asian Earth Sci 31:1–17

Adabi MH, Zohdi A, Ghabeishavi A, Amiri-Bakhtiyar H (2008) Applications of nummulitids and other larger benthic foraminifera in depositional environment and sequence stratigraphy: an example from the Eocene deposits in Zagros Basin, SW Iran. Facies 54:499–512. https://doi.org/10.1007/s10347-008-0151-7

Adams AE, MacKenzie WS (1998) A colour atlas of carbonate sediments and rocks under the microscope. Manson Publishing Limited, London

Afzal J, Butt AA (2000) Lower Tertiary planktonic biostratigraphy of the Salt Range, Northern Pakistan. Neues Jahrbuch Geol Palaont Mh 12:721–747

Ahmad N, Ahsan N, Sameeni SJ, Mirag MAF, Khan B (2013) Sedimentology and reservoir potential of the lower Eocene Sakesar limestone of Dandot Area, Eastern Salt Range, District Chakwal, Pakistan. Sci Int (Lahore) 25:521–529

Ahr WM (2008) Geology of carbonate reservoirs: the identification, description, and characterization of hydrocarbon reservoirs in carbonate rocks. Wiley, New Jersey

Alsharhan AS, Sadd JL (2000) Stylolites in lower Cretaceous carbonate reservoir, UAE. In: Alsharhan AS, Scott RW (eds) Middle East models of Jurassic/Cretaceous carbonate systems. SEPM Special Publication, vol 69, pp 179–200

Andre G (2003) Caractérisation des déformations méso-cénozoïques et des circulations de fluides dans l'Est du Bassin de ParisCharacterisation of the meso-cenozoic deformations and fluid circulations in the Eastern Paris Basin. Université Henri Poincaré-Nancy I, Français

Andrews LM, Railsback LB (1997) Controls on stylolite development: morphologic, lithologic, and temporal evidence from bedding-parallel and transverse stylolites from the US Appalachians. J Geol 105:59–73

Anketell JM, Mriheel IY (2000) Depositional environment and diagenesis of the Eocene Jdeir Formation, Gabes-Tripoli Basin, western offshore Libya. J Petrol Geol 23:425–447

Barattolo F, Bassi D, Romano R (2007) Upper Eocene larger foraminiferal–coralline Algal facies from the Klokova Mountain (southern continental Greece). Facies 53:361–375

Baron M, Parnell J (2007) Relationships between stylolites and cementation in sandstone reservoirs: examples from the North Sea, UK and East Greenland. Sediment Geol 194:17–35

Bathurst RGC (1975) Carbonate sediments and their diagenesis (developments in sedimentology 12). Elsevier, Amsterdam

Beavington-Penney SJ, Racey A (2004) Ecology of extant nummulitids and other larger benthic foraminifera: applications in palaeoenvironmental analysis. Earth-Sci Rev 67:219–265

Beavington-Penney SJ, Wright VP, Racey A (2006) The middle Eocene Seeb Formation of Oman: an investigation of acyclicity, stratigraphic completeness, and accumulation rates in shallow marine carbonate settings. J Sediment Res 76:1137–1161

Behl RJ (2011) Chert spheroids of the Monterey Formation, California (USA): early-diagenetic structures of bedded siliceous deposits. Sedimentology 58:325–351

Ben-Itzhak LL, Aharonov E, Karcz Z, Kaduri M, Toussaint R (2014) Sedimentary stylolite networks and connectivity in Limestone: large-scale field observations and implications for structure evolution. J Struct Geol 63:106–123

Berger S, Kaever MJ (1992) Dasycladales, an illustrated monograph of a fascinating Algal order

Blatt H, Middleton G, Murray R (1980) Origin of sedimentary rocks. Prince-Hall Inc, New Jersey, p 782

Boustani M, Khwaja AA (1997) Microfacies studies of Skaesar Limestone Central Salt Range, Pakistan. Geol Bull Univ Peshawar 30:131–142

Brandano M, Frezza V, Tomassetti L, Cuffaro M (2009) Heterozoan carbonates in oligotrophic tropical waters: the Attard member of the lower coralline limestone formation (Upper Oligocene, Malta). Palaeogeogr Palaeoclimatol Palaeoecol 274:54–63

Brigaud B, Durlet C, Deconinck J-F, Vincent B, Thierry J, Trouiller A (2009) The origin and timing of multiphase cementation in carbonates: impact of regional scale geodynamic events on the Middle Jurassic Limestones diagenesis (Paris Basin, France). Sediment Geol 222:161–180

Buxton M, Pedley H (1989) Short paper: a standardized model for Tethyan Tertiary carbonate ramps. J Geol Soc 146:746–748

Cantrell DL, Hagerty R (2003) Reservoir rock classification, arab-d reservoir, ghawar field, Saudi Arabia. GEOARABIA-MANAMA- 8:435–462

Carols L (2002) Diagenetic history of the Upper Jurassic Smackover formation and its effects on reservoir properties: vocation field, Manila Sub-Basin, Eastern Gulf Coastal Plain. Gulf Coast Assoc Geol Soc Trans 52:631–644

Davies LM, Pinfold ES (1937) The Eocene beds of the Punjab Salt Range. Indian Geol Surv Mem New Series 24:1–79

Dodd JR, Stanton RJ (1981) Paleoecology: concepts and Applications. Wiley & sons, Bloomington

Dunham RJ (1962) Classification of carbonate rocks according to depositional texture. In: Ham WE (ed) Classification of carbonate rocks. Memoir American Association of Petroleum Geologists, vol 1, pp 108–121

Ehrenberg S, Eberli G, Keramati M, Moallemi S (2006) Porosity-permeability relationships in interlayered limestone-dolostone reservoirs. AAPG Bull 90:91–114

Ehrenberg SN, Walderhaug O, Bjorlykke K (2012) Carbonate porosity creation by mesogenetic dissolution: reality or illusion? AAPG Bull 96:217–233

Esrafili-Dizaji B, Rahimpour-Bonab H (2009) Effects of depositional and diagenetic characteristics on carbonate reservoir quality: a case study from the South Pars gas field in the Persian Gulf. Petrol Geosci 15:325–344

Ferket H, Ortuo-Arzate S, Roure F, Swennen R (2003) Lithologic control on matrix porosity in shallow-marine cretaceous reservoir limestones: a study of the Peuela Reservoir Outcrop Analogue (Cordoba Platform, Southeastern Mexico). In: Bartolini C, Buffler RT, Blickwede J (eds) The circum-Gulf of Mexico and the Caribbean: hydrocarbon habitats, basin formation, and plate tectonics. AAPG Memoir, vol 79, pp 283–304

Flügel E (2010) Microfacies of carbonate rocks: analysis, interpretation and application, 2nd edn. Springer, Berlin. https://doi.org/10.1007/978-3-642-03796-2

Gee ER (1980) Salt Range series geological maps: Directorate of Overseas Surveys, United Kingdom, for Government of Pakistan and Pakistan Geological Survey, 1:50,000, 6 sheets

Gee E, Gee D (1989) Overview of the geology and structure of the Salt Range, with observations on related areas of northern Pakistan. Geol Soc Am Special Pap 232:95–112

Geel T (2000) Recognition of stratigraphic sequences in carbonate platform & slope deposits: empirical models based on moicrofacies analysis of Palaeogene deposits in south-eastern Spain. Palaeogeogr Palaeoclimatol Palaeoecol 155:211–238

Ghazi S, Ali SH, Sahraeyan M, Hanif T (2015) An overview of tectonosedimentary framework of the Salt Range, northwestern Himalayan fold and thrust belt, Pakistan. Arab J Geosci 8:1635–1651

Ghazi S, Butt AA, Ashraf M (2006) Microfacies analysis and diagenesis of the Lower Eocene Sakesar Limestone, Nilawahan Gorge, central Salt Range, Pakistan. J Nepal Geol Soc 33:23–32

Ghazi S, Ahmad S, Zeb N, Sharif S, Akhtar S (2010) Sedimentology, microfacies analysis and diagenesis of the Lower Eocene the Sakesar Limestone, central Salt Range, Pakistan. J Nepal Geol Soc 41:23

Gilham RF, Bristow CS (1998) Facies architecture and geometry of a prograding carbonate ramp during the early stages of foreland basin evolution: lower Eocene sequences, Sierra del Cadí, SE Pyrenees, Spain. Geol Soc Lond Spec Publ 149:181–203

Granier B (2012) The contribution of calcareous green algae to the production of limestones: a review. Geodiversitas 34:35–60

Hallock P (1985) Why are larger foraminifera large? Paleobiology 11:195–208

Harris MK, Thayer PA, Amidon MB (1997) Sedimentology and depositional environments of middle Eocene terrigenous-carbonate strata, southeastern Atlantic Coastal Plain, USA. Sediment Geol 108:141–161

Hassan HM (2007) Stylolite effect on geochemistry, porosity and permeability: comparison between a limestone and a dolomite sample from Khuff-B reservoir in Eastern Saudi Arabia. Arab J Sci Eng 32:139

Heckel PH (1972) Possible inorganic origin for Stromatactis in calcilutite mounds in the Tully Limestone, Devnonian of New York. J Sediment Petrol 42:7–18

Hohenegger J (2000) Coenoclines of larger foraminifera. Micropaleontology 46:127–151

Hohenegger J (2004) Depth coenoclines and environmental considerations of western Pacific larger foraminifera. J Foraminifer Res 34:9–33

Hohenegger J, Yordanova E, Nakano Y, Tatzreiter F (1999) Habitats of larger foraminifera on the upper reef slope of Sesoko Island, Okinawa, Japan. Mar Micropaleontol 36:109–168

Höntzsch S, Scheibner C, Kuss J, Marzouk AM, Rasser MW (2011) Tectonically driven carbonate ramp evolution at the southern Tethyan shelf: the Lower Eocene succession of the Galala Mountains, Egypt. Facies 57:51–72

Hottinger L (1997) Shallow benthic foraminiferal assemblages as signals for depth of their deposition and their limitations. Bull de la Société géologique de France 168:491–505

Jadoon IAK, Bhatti KM, Siddiqui FI, Jadoon SK, Gilani SRH, Afzal M (2005) Subsurface fracture analysis in Carbonate Reservoirs: Kohat/Potwar Plataeu, north Pakistan. Paper presented at the SPE/PAPG annual Technical Conference, Islamabad, November, 28–29, 2005

Jadoon IAK, Frisch W, Jadoon MSK (2008) Structural traps and hydrocarbon exploration in the Salt Range/Potwar Plateau, North Pakistan. In: SPE Annual Technical Conference, Islamabad, pp 69–83

Jan IU, Stephenson MH (2011) Palynology and correlation of the Upper Pennsylvanian Tobra Formation from Zaluch Nala, Salt Range, Pakistan. Palynology 35:212–225

Jaswal TM, Lillie RJ, Lawrence RD (1997) Structure and Evolution of the Northern Potwar Deformed Zone, Pakistan. AAPG Bull 81:308–328

Kazmi AH, Jan MQ (1997) Geology and tectonics of Pakistan. Graphic Publishers, Karachi

Kennedy M (2015) Practical petrophysics, vol 62. Developments in Petroleum Science, Elsevier, Amsterdam

Khalifa M (2005) Lithofacies, diagenesis and cyclicity of the 'lower member'of the Khuff formation (late Permian), Al Qasim Province, Saudi Arabia. J Asian Earth Sci 25:719–734

Khalifa M, Kumon F, Yoshida K (2009) Calcareous duricrust, Al Qasim Province, Saudi Arabia: occurrence and origin. Q Int 209:163–174

Khan AM, Ahmed R, Raza HA, Kemal A (1986) Geology of petroleum in Kohat—Potwar depression, Pakistan. AAPG Bull 70:396–414

Larsen B, Grunnaleite I, Gudmundsson A (2010) How fracture systems affect permeability development in shallow-water carbonate rocks: an example from the Gargano Peninsula, Italy. J Struct Geol 32:1212–1230

Logan BW (1984) Pressure responses (deformation) in carbonate sediments and rocks—analysis and application, Canning Basin. In: Purcell PG (ed) The Canning Basin, W.A., Perth. In: Proceedings of the Geological Society of Western Australia/Petroleum Exploration Society of Australia, pp 235–251

Loucks R, Moody R, Bellis J, Brown A (1998) Regional depositional setting and pore network systems of the El Garia Formation (Metlaoui Group, Lower Eocene), offshore Tunisia. Geol Soc Lond Spec Publ 132:355–374

Loucks RG, Reed RM, Ruppel SC, Hammes U (2012) Spectrum of pore types and networks in mudrocks and a descriptive classification for matrix-related mudrock pores. AAPG Bull 96:1071–1098

Macintyre IG, Reid RP (1995) Crystal alteration in a living calcareous alga (Halimeda): implications for studies in skeletal diagenesis. J Sediment Res 65:143–153

Mahboubi A, Moussavi-Harami R, Carpenter SJ, Aghaei A, Collins LB (2010) Petrographical and geochemical evidences for paragenetic sequence interpretation of diagenesis in mixed siliciclastic–carbonate sediments: mozduran Formation (Upper Jurassic), south of Agh-Darband, NE Iran. Carbonates Evaporites 25:231–246

Mehr MK, Adabi MH (2014) Microfacies and geochemical evidence for original aragonite mineralogy of a foraminifera-dominated carbonate ramp system in the late Paleocene to Middle Eocene, Alborz basin, Iran. Carbonates Evaporites 29:155–175

Melim LA, Swart PK, Maliva RG (2001) Meteoric and marine burial diagenesis in the subsurface of the Great Bahama Bank. In: Ginsburg, RN (ed) Subsurface geology of a prograding Carbonate Platform Margin, Great Bahama Bank. SEPM Spec Publ, vol 70, pp 137–162

Melim L, Westphal H, Swart P, Eberli G, Munnecke A (2002) Questioning carbonate diagenetic paradigms: evidence from the Neogene of the Bahamas. Mar Geol 185:27–53

Morad S, Al-Aasm IS, Nader FH, Ceriani A, Gasparrini M, Mansurbeg H (2012) Impact of diagenesis on the spatial and temporal distribution of reservoir quality in the Jurassic Arab D and C members, offshore Abu Dhabi oilfield, United Arab Emirates. GeoArabia 17:17–56

Moradpour M, Zamani Z, Moallemi S (2008) Controls on reservoir quality in the lower Triassic Kangan formation, southern Persian Gulf. J Petrol Geol 31:367–385

Mujtaba M, Abbas G (2001) Diagenetic control on porosity development in the early Eocene carbonate reservoirs of Potwar Sub-Basin, Pakistan. Pak J Hydrocarb Res 12:65–72

Nader FH (2017) Introduction. In: Multi-scale quantitative diagenesis and impacts on heterogeneity of Carbonate Reservoir Rocks. Springer, New York, pp 1–13

Nenna F, Aydin A (2011) The formation and growth of pressure solution seams in clastic rocks: a field and analytical study. J Struct Geol 33:633–643

Nizami AR, Qayyum A, Shahbaz A, Bhatti ZI, Pirzada TS (2010) Microfacies assemblages and diagenetic framework of the Lower Eocene Sakesar limestone, Karoli area, Central Salt Range, Sub-Himalayas of Pakistan. J Himal Earth Sci 43:66–66

Noble J, Van Stempvoort D (1989) Early burial quartz authigenesis in Silurian platform carbonates, New Brunswick, Canada. J Sediment Petrol 59:65–76

Oswald E, Mueller III H, Goff D, Al-Habshi H, Al-Matroushi S (1995) Controls on porosity evolution in Thamama Group carbonate reservoirs in Abu Dhabi, UAE. Paper presented at the Middle East Oil Show

Paganoni M, Al Harthi A, Morad D, Morad S, Ceriani A, Mansurbeg H, Al Suwaidi A, Al-Aasm IS, Ehrenberg SN, Sirat M (2016) Impact of stylolitization on diagenesis of a Lower Cretaceous carbonate reservoir from a giant oilfield, Abu Dhabi, United Arab Emirates. Sediment Geol 335:70–92

Park WC, Schot EH (1968) Stylolites: their Nature and Origin. J Sediment Petrol 38:175–191

Passchier CW, Trouw RAJ (2005) Microtectonics, 2nd edn. Springer, Berlin

Payros A, Pujalte V, Tosquella J, Orue-Etxebarria X (2010) The Eocene storm-dominated foralgal ramp of the western Pyrenees (Urbasa–Andia Formation): an analogue of future shallow-marine carbonate systems? Sediment Geol 228:184–204

Puga-Bernabéu A, Martín JM, Braga JC, Sánchez-Almazo IM (2010) Downslope-migrating sandwaves and platform-margin clinoforms in a current-dominated, distally steepened temperate-carbonate ramp (Guadix Basin, Southern Spain). Sedimentology 57:293–311

Racey A (1994) Biostratigraphy and palaeobiogeographic significance of Tertiary nummulitids (Foraminifera) from northern Oman. In: Simmons MD (ed) Micropalaeontology and hydrocarbon exploration in the Middle East. Chapman and Hall, London, pp 343–370

Racey A (2001) A review of Eocene nummulite accumulations: structure, formation and reservoir potential. J Pet Geol 24:79–100. https://doi.org/10.1111/j.1747-5457.2001.tb00662.x

Rasser MW, Scheibner C, Mutti M (2005) A paleoenvironmental standard section for Early Ilerdian tropical carbonate factories (Corbieres, France; Pyrenees, Spain). Facies 51:218–232

Reeckmann A, Friedman GM (1982) Exploration for Carbonate Petroleum Reserviors. Wiley, New Yark

Richter D, Götte T, Götze J, Neuser R (2003) Progress in application of cathodoluminescence (CL) in sedimentary petrology. Mineral Petrol 79:127–166

Rolland A, Toussaint R, Baud P, Conil N, Landrein P (2014) Morphological analysis of stylolites for paleostress estimation in limestones. Int J Rock Mech Mining Sci 67:212–225

Sameeni SJ, Butt AA (2004) Alveolinid biostratigraphy of the Salt Range succession, Northern Pakistan. Revue Paleobiologie 23:505–527

Sarwar G, DeJong KA (1979) Arcs, oroclines, syntaxes: the curvature of mountain belts in Pakistan. In: Farah A, DeJong KA (eds) Geodynamics of Pakistan. Geol Surv Pak, Quetta, pp 341–358

Scheibner C, Rasser MW, Mutti M (2007) Facies changes across the Paleocene-Eocene boundary: the Campo section (Pyrenees, Spain) revisited. Palaegeogr Palaeoclimatol Palaeoecol 248:145–168

Selley RC (2000) Applied sedimentology. Elsevier, Amsterdam

Shami BA, Baig MS (2002) Geomodelling for the enhancement of hydrocarbon potential of Joya Mair Oil Field, Potwar, Pakistan SPE/PAPG Annual Technical Conference, Islamabad, pp 124–145

Sinclair H, Sayer Z, Tucker M (1998) Carbonate sedimentation during early foreland basin subsidence: the Eocene succession of the French Alps. Geol Soc London Spec Publ 149:205–227

Spence GH, Finch E (2014) Influences of nodular chert rhythmites on natural fracture networks in carbonates: an outcrop and two-dimensional discrete element modelling study. Geol Soc Lond Spec Publ 374:211–249

Swei G, Tucker ME (2012) Impact of diagenesis on reservoir quality in ramp carbonates: Gialo Formation (Middle Eocene), Sirt Basin, Libya. J Petrol Geol 35:25–47

Taghavi AA, Mørk A, Emadi MA (2006) Sequence stratigraphically controlled diagenesis governs reservoir quality in the carbonate Dehluran Field, southwest Iran. Petrol Geosci 12:115–126

Tavakoli V, Rahimpour-Bonab H, Esrafili-Dizaji B (2011) Diagenetic controlled reservoir quality of South Pars gas field, an integrated approach. Comptes Rendus Geosci 343:55–71

Tondi E, Antonellini M, Aydin A, Marchegiani L, Cello G (2006) The role of deformation bands, stylolites and sheared stylolites in fault development in carbonate grainstones of Majella Mountain, Italy. J Struct Geol 28:376–391

Tucker ME, Wright VP (1990) Carbonate sedimentology. Blackwells Scientific Pulications, Oxford

Vandeginste V, John CM (2013) Diagenetic implications of stylolitization in pelagic carbonates, Canterbury Basin, offshore New Zealand. J Sediment Res 83:226–240

Vaziri-Moghaddam H, Kimiagari M, Taheri A (2006) Depositional environment and sequence stratigraphy of the Oligo-Miocene Asmari Formation in SW Iran. Facies 52:41–51

Vincent B (2001) Sédimentologie et géochimie de la diagenèse des carbonates: application au Malm de la bordure Est du Bassin de Paris. Dijon University, Dijon

Vincent B, Emmanuel L, Houel P, Loreau J-P (2007) Geodynamic control on carbonate diagenesis: petrographic and isotopic investigation of the Upper Jurassic formations of the Paris Basin (France). Sediment Geol 197:267–289

Viti C, Collettini C, Tesei T (2014) Pressure solution seams in carbonatic fault rocks: mineralogy, micro/nanostructures and deformation mechanism. Contrib Mineral Petrol 167:1–15

Westphal H, Eberli GP, Smith LB, Grammer GM, Kislak J (2004) Reservoir characterization of the Mississippian Madison Formation, Wind River basin, Wyoming. AAPG Bull 88:405–432

Wilson M, Vecsei A (2005) The apparent paradox of abundant foramol facies in low latitudes: their environmental significance and effect on platform development. Earth-Sci Rev 69:133–168

Wray JL (1977) Calcareous algae. In: Haq BU, Boersma A (eds) Introduction to marine micropaleontology. Elsevier, North-Holland, pp 171–187

Wright V (1986) Facies sequences on a carbonate ramp: the Carboniferous Limestone of South Wales. Sedimentology 33:221–241